Microporous and Mesoporous Materials 291 (2020) 109698

Contents lists available at ScienceDirect

Microporous and Mesoporous Materials

journal homepage: www.elsevier.com/locate/micromeso

Recent progresses in the adsorption of organic, inorganic, and gas compounds by MCM-41-based mesoporous materials

José Arnaldo S. Costa[a,b,*], Roberta A. de Jesus[c], Danilo O. Santos[d], João F. Mano[a], Luciane P.C. Romão[d,e], Caio M. Paranhos[b]

[a] CICECO, Department of Chemistry, University of Aveiro, 3810-193, Aveiro, Portugal
[b] CDMF, Department of Chemistry, Federal University of São Carlos, 13565-905, São Carlos, São Paulo, Brazil
[c] Institute of Chemistry and Biotechnology, Federal University of Alagoas, 57072-970, Maceió, Alagoas, Brazil
[d] Department of Chemistry, Federal University of Sergipe, 49100-000, São Cristóvão, SE, Brazil
[e] Institute of Chemistry, UNESP, National Institute for Alternative Technologies of Detection, Toxicological Evaluation and Removal of Micropollutants and Radioactives (INCT-DATREM), 14800-900, Araraquara, SP, Brazil

ARTICLE INFO

Keywords:
Mesoporous material
MCM-41
Adsorption process
Pollutants
Environmental remediation

ABSTRACT

Adsorbent mesoporous materials are highly efficient for the remediation of different compounds in environmental applications such as organic, inorganic, and gas molecules. These compounds are removed by the traditional adsorption process in batch assessments. In this review, we report the recent progress on the MCM-41-based mesoporous material syntheses and its strategic use as an adsorbent material for the removal of different pollutants. Also approached the main factors that affect its synthesis and the methods of functionalization most used to prepare the MCM-41-based functionalized mesoporous materials. On the other hand, the factors that affect the adsorption process were also investigated. In addition, it is possible to affirm that adsorption technology has attracted a lot of attention in the removal of environmental pollutants, mainly due to the fact that it is a technique that requires the use of few steps and equipment, easy operation, low cost, does not generate residues or by-products, eco-friendly, and high energy efficiency, which allow its wide application on the remediation processes.

1. Introduction

In the last decades, there has been a significant increase in the area of nanotechnology and nanoscience regarding the synthesis, characterization, evaluation of properties and wide range of applications in catalysis, adsorption, separation, control of environmental pollution, controlled release of drugs, and sensors aiming at improvement of quality of daily life of society. One of the most promising classes of nanoscale materials are mesoporous silicates that have attracted the attention of several researchers because of their potential applications [1–7].

In the early 1990s scientists at Mobil Oil Corporation synthesized the first ordered mesoporous silicate materials which are known as the M41S family [7–9]. The term M41S is used to generalize the various types of MCM (Mobil Composition of Matter) synthesized under basic conditions in the presence of alkylammonium surfactants and a silica source whose pore size comprises the range of 3–10 nm [10]. The most well-known types of this class of materials include the MCM-41 (hexagonal structure, with space-group symmetry (*P*6mm) and unidirectional system of pores) [8,9], MCM-48 (cubic structure, with space-group symmetry (la3d) and pores interconnected in three-dimensional system) [9,11], and MCM-50 (lamellar structure, without space-group symmetry, consisting of silica layers in presence of double layers of surfactant [9,12]. Fig. 1 shows the schematic representation of mesoporous materials of M41S family.

In 1998, the Santa Barbara Amorphous family (SBA) composed of silica-based materials, with well-ordered mesopores, was synthesized in strong acid medium. The materials discovered include the SBA-2 (hexagonal close-packed array), SBA-12 (three-dimensional hexagonal network), SBA-14 (cubic structure), SBA-15 (two-dimensional hexagonal), and SBA-16 (structured in cubic cage) [13,14]. SBA-15 is the family member widely reported in the literature, due to its structural and textural features presented in the synthetized mesoparticles (with uniform pores of up to 30 nm) [15–18]. Fig. 2 shows the schematic representation of SBA-15 mesoporous material.

Mesoporous materials synthesized under neutral conditions with

* Corresponding author. CICECO, Department of Chemistry, University of Aveiro, 3810-193, Aveiro, Portugal.
E-mail address: josearnaldo@ua.pt (J.A.S. Costa).

https://doi.org/10.1016/j.micromeso.2019.109698
Received 17 July 2019; Received in revised form 15 August 2019; Accepted 2 September 2019
Available online 03 September 2019
1387-1811/

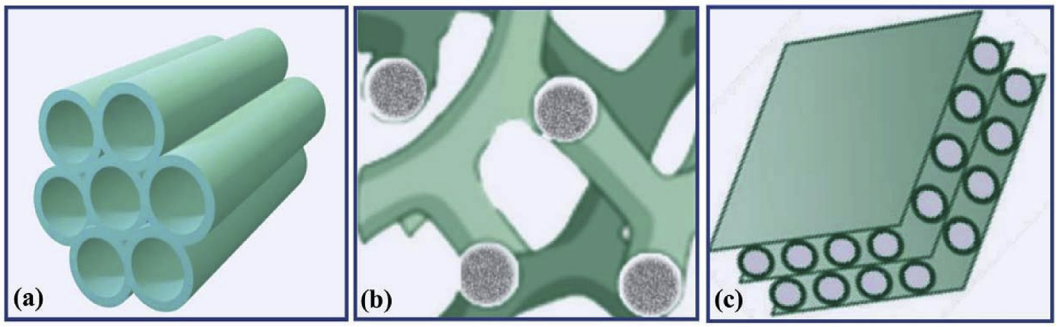

Fig. 1. Schematic representation of the structure of MCM-41 (a), MCM-48 (b), and MCM-50 (c) mesoporous materials of M41S family.

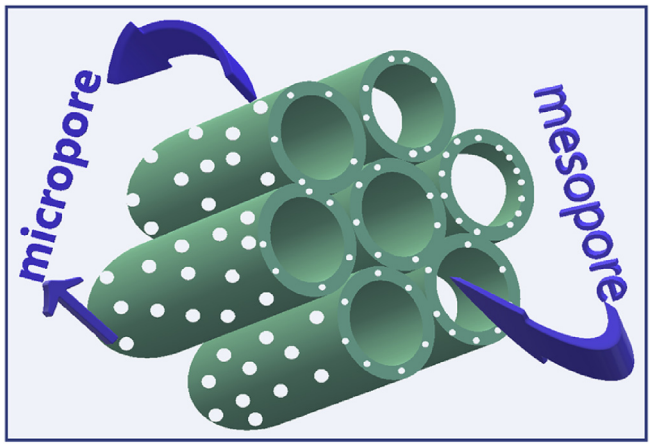

Fig. 2. Schematic representation of the structure of SBA-15 mesoporous material.

non-ionic surfactants were first developed at Michigan State University and are referred to as MSU-X, where X represents a number for distinguishing different MSU materials. These materials have disorganized structures in relation to materials of M41S and SBA families and their pore diameter and wall thickness are at around 2.1–8.0 nm and 1.5–4.0 nm, respectively. Finally, other important materials are prepared by the addition of a swelling agent to the synthesis of SBA-15 which exhibits 3D foam sponge structure and large pore volumes. They are referred to as mesostructured cellular foam (MCF) [19].

1.1. The history of the M41S family of mesoporous materials

Zeolites are members of a large family of ordered aluminosilicates. They were discovered in 1756 by the Swedish mineralogist Cronstedt when heating an unidentified silicate mineral. Only in 1926, the adsorption characteristics of zeolites (in particular chabazite) were attributed to small pores of about 5 Å in diameter [20]. The attractive trade in zeolite materials with small pore diameters is due to their potential for selective adsorption of small gaseous molecules, such as nitrogen and oxygen, which can be selectively separated [21].

Despite attracting much attention and scientific importance, the zeolites did not find any significant application due to their inherent weak stability, poor acidity, and small pore size (0.8–1.3 nm). In this context, there was a growing interest in the synthetic development of zeolites with adjustable pore size for applications in various areas, such as industrial, separation, adsorption, and catalytic purposes. As a result of these studies, the first synthesis of MCM-41 mesoporous material was reported in 1992 [7–9].

The term molecular sieve was derived from McBain in 1932, since it is used to describe a class of materials which exhibit selective sorption properties. These materials are able to selectively separate a mixture from the distinction of size and shape molecular of the compounds. Thus, the zeolites and MCM-41 are characterized as molecular sieves [22]. According to the IUPAC definition, porous materials are divided into three classes depending of pore size: microporous (pore diameter < 2 nm), mesoporous (pore diameter between 2 and 50 nm), and macroporous (pore diameter > 50 nm) [23].

There was, however, a growing interest in the expansion of pore sizes of zeolite materials from the microporous region to the mesoporous region due to the increasing demand in industrial applications [24–26]. Despite some unsuccess attempts, only in 1982 was obtained the first so-called ultra-large pore molecular sieve, designated $AlPO_4$-8, containing 14-membered rings [27,28]. In fact, this not only surpassed the traditional point of view that the molecular sieves of zeolite could not be constructed with more than 12 ring members, but also stimulated investigations in other ultra-large pore molecular sieves such as VPI-5 with an opening of 18 tetrahedral rings, among others [24,29,30].

In the early 1990s, Yanagisawa and collaborators synthesized mesoporous materials with characteristics similar to MCM-41 [31]. The methodological procedure was based on the long chain intercalation of alkyltrimethylammonium cations (typically C-16) into the layered silicate kanemite, followed by calcination to remove the organic compounds (surfactant). The preparation mechanism promoted a condensation of silicate layers and the formation of three-dimensional nanoscale porous structures. The success of the synthesis was confirmed by the ^{29}Si solid state NMR spectroscopy analysis, which indicated complete condensation of silica during the intercalation and calcination processes. On the other hand, the results reported by Yanagisawa and collaborators were not considered relevant due to the absence of corroborative characterization data.

Molecular sieves of M41S family consisting of silicate/aluminosilicate were discovered in 1992 by researchers from Mobil Oil Corporation [7,8]. In general, these materials are prepared from the sol-gel process and use of a template. Three well-defined structural arrangements were identified after studying the effect of surfactant concentration in the prepared mesoparticles: hexagonal structure (MCM-41), cubic structure (MCM-48), and lamellar structure (MCM-50) as shown in Fig. 1. Thus, the mesoporous molecular sieves of M41S family exhibit structural and textural characteristics that are quite different from those observed for zeolite materials. The mesoporous arrays contain little or no Brønsted acidity in their amorphous walls of about 10 Å. These thin amorphous walls can be a possible limitation for the thermal and hydrothermal stability of mesoparticles under some severe conditions. However, the structural ordering of mesoporous materials can be conserved with increasing hydrothermal synthesis temperature and/or time [9]. Due to these properties, M41S molecular sieves have attracted great attention in the catalysis area [6,32–34], separation [27,35], adsorption [36–45], sensor [46,47], and controlled release of drugs [33,48,49].

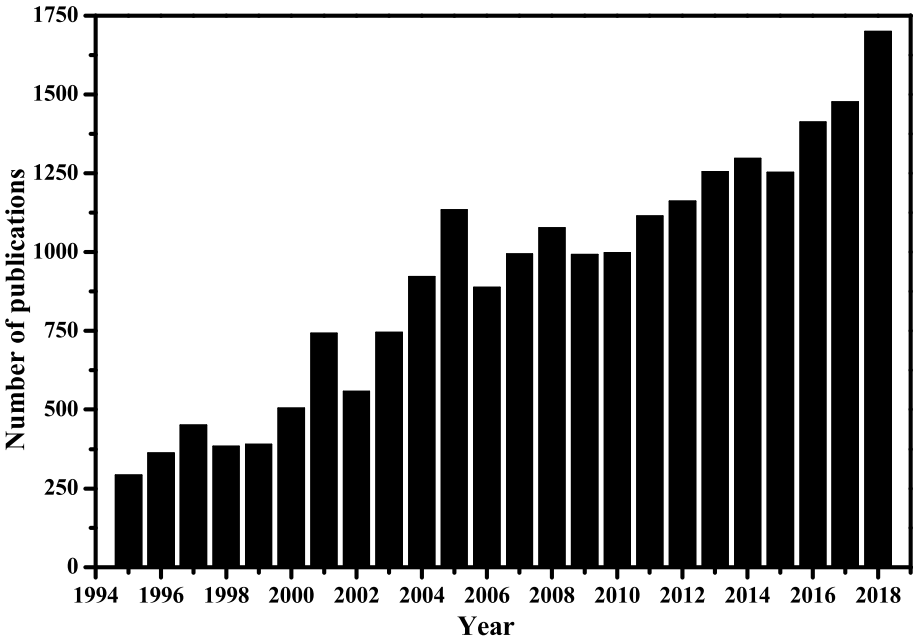

Fig. 3. Evolution of the number of publications of MCM-41-based mesoporous materials.

1.2. MCM-41-based mesoporous materials

According to the results obtained in the Science Direct database from 1994 to 2018 (Fig. 3), various studies have been published with mesoporous materials of M41S family. Nevertheless, MCM-41 has been the most investigated mesoporous material because the other members of this family are thermally unstable or difficult to obtain.

MCM-41-based mesoporous materials are composed of amorphous silica with large pores in the form of cylindrical channels. The pore diameter of mesoparticles can vary in the range of 1–10 nm, and MCM-41 has a high surface area around 1000 $m^2 g^{-1}$ and pore volumes greater than 0.5 mL g^{-1}. It presents good thermal, hydrothermal, and hydrolytic stability [34,50]. Due to these properties, the MCM-41 has attracted great attention especially in the area of adsorption.

MCM-41-based mesoporous materials can be prepared by a variety of synthetic routes. However the conventional method most used is hydrothermal one in a poly(tetrafluorethylene)-lined stainless steel autoclave [51]. Alternatively, the preparation of mesoparticles have been successful by microwave irradiation [52,53]. The advantage of microwave irradiation is that this method allows higher yields, high purity, and higher rate of crystallization reaction when compared to the hydrothermal method [54]. Both methods are basically performed with a silica source [tetraethylorthosilicate (TEOS), silica gel, colloidal silica, sodium silicate or other], a porosity controlling agent that can be a cationic, anionic or neutral surfactant and, finally, water as solvent. Afterwards, the pH is adjusted and the solution is heated by hydrothermal or microwave irradiation [36,37,48,55]. The final step of synthesis consists of calcination or extraction of obtained mesoporous material which gives high crystallinity and removal of the residual surfactant after washing the structure.

This mesoporous material can be characterized by different techniques such as transmission electron microscopy (TEM), scanning electron microscopy (SEM), X-ray diffraction (XRD) or small-angle X-ray scattering (SAXS), N_2 adsorption-desorption, and Fourier transform medium-infrared spectroscopy (FTIR). The TEM provides information with higher resolution of the morphology of mesoparticles, while the SEM provides information of lower morphology resolution [56,57]. XRD or SAXS shows the crystal structure changes of MCM-41 caused by variations in synthetic parameters. The crystallographic mesopattern presents four indexed peaks (h, k, l) with decreasing intensity (100), (110), (200), and (210) characteristic of mesoporous materials with well-defined hexagonal network arrangement (MCM-41) [58,59].

The FTIR presents some typical absorption bands useful in MCM-41 characterization: stretching of OH bonds of adsorbed water molecules within the mesoporous matrix, as well as the stretching of silane groups (Si–OH) (3435 cm^{-1}); flexion of OH bonds from water molecules (1647 cm^{-1}); asymmetric Si–O–Si vibrations (1085 cm^{-1}); symmetric Si–O–Si vibrations (802 cm^{-1}); bending of Si–O–Si (470 cm^{-1}) [38]. The efficiency of calcination or extraction process of template is seen by the absence of bands related to the organic surfactant in the surface of mesoparticles.

The surface area, pore diameter and volume of mesoporous material are determined by the study of nitrogen adsorption-desorption isotherms. The surface area is usually calculated using the relative pressure data by the Brunauer-Emmett-Tellet (BET) method [60]. On the other hand, the pore volume and size distribution are usually determined using the Barrett-Joyner-Halenda (BJH) method [61]. According to the IUPAC classification, most of mesoporous solids present one of the six types of adsorption isotherms. MCM-41 presents type IV isotherm with a marked increase in the volume of nitrogen adsorbed at the mean relative pressure (P/P_o) [38]. In the type IV isotherm occurs initially to the cover of a monolayer, the second layer of adsorption indicates the band of mesoporous of mesoporous matrix. The uniformity of pore diameters influences the occurrence or absence of hysteresis loop and the isotherm does not follow the same path for adsorption and desorption. Currently, IUPAC classifies six types of hysteresis loops [H1, H2(a), H2(b), H3, H4, and H5]. Each of these six types is reasonably related to certain characteristics of porous structure and underlying adsorption mechanism. Type H1 hysteresis is found in mesoparticles which exhibit a narrow range of uniform mesopores, such as MCM-41, MCM-48, and SBA-15. Normally, the network effects are minimal and the steep and narrow circuit is a clear signal of delayed condensation in the adsorption branch [62].

2. Methods of synthesis

In the preparation of MCM-41-based mesoporous material, four reactants are essential, such as the silica source, a mineralizing agent, a solvent, and a template (it is responsible for forming the pores of mesoparticles). MCM-41 can be synthesized from a variety of methods

with distinct silica sources, surfactants, experimental conditions such as time, temperature, and pH [63]. In general, MCM-41 is prepared in the presence of a directing agent and a silica source. A mineralizing agent (sodium hydroxide or ammonium solution) is used to dissolve the silica and form silicate ions [64]. The high surface area, high thermal stability, and specific pore size distribution are favorable characteristics for the various applications of MCM-41-based mesoporous materials. Their physical structures are highly controllable from the desired properties, such as composition variations of solutions, concentrations, and temperature. Variations in the synthesis parameters alter some structures of mesoparticles, such as surface area, pore diameter, center-center distance, and pore size [65].

Experimental conditions are determinant factors for the properties of MCM-41, since the condensation of silanol groups is influenced by the pH of reaction medium. In basic media, the preparation presents better condensation results of silanol groups, resulting in a well-ordered structure that provides high surface area. However, in acid media, there is better variation of morphological forms of mesoparticles [66]. Lin et al. [67] studied the presence of other bases instead of NaOH [68] and tetramethylammonium hydroxide [7,8]. The methylamine, dimethylamine, ethylamine, and diethylamine bases in water were tested and showed higher surface areas and hydrothermal stability when compared to the materials synthesized with NaOH. On the other hand, Huo et al. [69] synthesized the MCM-41 in acid medium, with the presence of HCl and HBr in concentrations ranging from 5 to 9 mol L^{-1}. The results demonstrate that the textural properties were consistent with the mesoporous materials produced in basic media. Whole Silva et al. [70] presented a study of the synthesis of MCM-41 in fluoride medium. In this work, the mesoparticles were prepared using sodium silicate, surfactant, and water. The results obtained showed that the mesoporous material produced had high mesoporous arrangement and a high surface area between 1000 and 1100 $m^2 g^{-1}$.

Some techniques are being used to increase the hydrothermal stability of MCM-41 mesoparticles prepared. Zhai et al. [71] incorporated Al to the material with the addition of $NaAlO_2$ solution in the reaction mixture, resulting in considerably increase in the acidity on the surface of final product. While Tompkins and Mokaya [72] were able to thermally stabilize Al-MCM-41 with the addition of trace amounts of Al by the dry grafting method, Carrott et al. [73] prepared thermally stable Ti-MCM-41 materials with different Ti contents, and Lysenko et al. [74] increased stability and acidity of MCM-41 from the MCM-41/γ-Al_2O_3 catalytic support in the presence of pseudoboehmite and modification with metal ions. On the other hand, Zhao and Lu [75] removed silanol groups by silylation using trimethylchlorosilane. The results showed that the surface chemistry was altered with the modification and the pore diameter was significantly reduced by silylation. Zhao et al. [76] reported the preparation of thicker pore walls and uniform materials from the use of amphiphilic triblock copolymer. Shi-quan et al. [77] presented different routes for pore engineering of spherical MCM-41 including hydrothermal post-synthesis treatment that resulted in better hydrothermal stability of mesoparticles produced. The use of expanders in the synthesis of MCM-41 causes structural modifications in their mesoparticles. These agents are voluminous organic molecules that are added in the reaction medium to increase the pore diameter, but result in low chemical and hydrothermal stability [78].

The MCM-41-based mesoporous materials can be synthesized from different methods such as sol-gel process [67], microwave heating [79], and hydrothermal processing [80]. The conventional method used in the preparation of MCM-41 is the hydrothermal processing with the reagents placed in a poly(tetrafluorethylene)-lined stainless steel autoclave. Originally, MCM-41 was synthesized with the mixture of water, sodium silicate, and sulfuric acid under stirring. The resulting mixture was added to the surfactant $C_{16}H_{33}(CH_3)_3NOH/Cl$ to form a gel which was stirred for 0.5 h. Water was added to the gel and the mixture heated at 100 °C for 144 h. The resulting solid was washed with water, filtered, and calcined for template removal [8,81]. Ortiz et al. [82] presented a study of the hydrothermal synthesis of MCM-41 with variations of reaction conditions, such as material composition, temperature, and reaction time. The authors found the following conditions to be the best: CTAB/SiO_2 molar ratio from 0.53 to 0.71, reaction time of 110 h and temperature of 80 °C.

An alternative method is microwave irradiation [52,79]. According to Park et al. [52], this procedure achieves higher yields, better purity, higher reaction rate, and crystallization when compared to the conventional method. MCM-41 mesoparticles can be obtained by microwave treatment of precursor gel at 100 °C for 1 h, less time compared to the conventional method. In addition, the authors reported that the addition of small amounts of ethylene glycol improves crystallinity by reducing mesoparticle size.

On the other hand, Yilmaz et al. [43] reported the preparation of MCM-41 mesoparticles by the classical (hydrothermal) method and by ultrasound. For the ultrasound method, 35 kHz ultrasound was used for 1 h at 50 °C in basic medium. The mesoporous material was formed in both methods. However, the mesoparticles synthesized by the classical method presented higher surface area, pore volume, and coherent unit cell parameters.

A common feature in all synthetic routes is the presence of a directing agent, surfactant or template. A director is an agent that guides the structure during synthesis, since the mesoparticles are formed around it. The most common conductors are quaternary ammonium ions with long alkyl chains that enable the formation of rod-shaped tubes during the preparation of MCM-41 mesoporous material. The driver is an organic molecule that has in its structure a polar (hydrophilic) and an apolar (hydrophobic) end composed of a hydrocarbon chain. The most common surfactant in the literature is cetyltrimethylammonium bromide (CTAB) used in basic media [83,84].

Schmidt et al. [39] reported the production of three samples of MCM-41 mesoparticles with different pore sizes of 18, 27, and 40 Å. To obtain variations in the pore size, the authors used different targeting agents: $C_{14}H_{29}(CH_3)NBr$ (sample 1 and 2) and $C_8H_{17}(CH_3)_3NBr$ (sample 3). In sample 1, mesitylene was added. Sample 1 had the largest pore size and surface area close to that of sample 2. The smallest pore size and surface area was found for sample 3. In this way, it is suggested that conducting agents with higher carbon chains will result in larger pore size of materials. Feuston and Higgins [85] showed that the decrease in pore size promoted by the choice of guiding agent increases the wall thickness of MCM-41.

In the preparation of MCM-41, the directing agent, depending on the application, must be removed prior to the use of material. In most cases, the synthesized mesoporous materials are thermally treated for removal in the presence of oxygen or air above 550 °C. Other alternative methods have already been successfully tested, such as solvent extraction [86–89] and methods with microwaves [90]. The removal of directing agent is a necessary process for the generation of pores and to provide some properties to the material uses, such as catalysts [91] and adsorption [37]. A technique used for this purpose is calcination [92]. Kruk et al. [93] studied the structure of MCM-41 with guider and calcined. Comparison of the data allowed to exclude the possibility of any appreciable structural degradation during calcination, suggesting that it is an effective means to remove the template from the mesoporous structure. In addition, calcination provides a consolidation of the formed hexagonal structure [94]. However, there are studies reporting that this process can lead to local defects and collapses the mesoparticle structure [95,96]. In order to avoid such situations, the solvent extraction method is a non-destructive proposal to remove the template of internal structure of mesoparticles [86,87].

Marcilla et al. [97] presented a study with three ways of template removal: calcination and two distinct extraction processes, one with ethanol and another with H_2O_2. The results suggest that the three samples exhibit acceptable textural and structural properties. However, mesoparticles treated with a HCl/Ethanol mixture causes structure damage depending of experimental conditions, suggesting that

hydrogen peroxide treatment is the best route for template removal.

There is a wide variety of methods for the preparation of MCM-41-based mesoporous materials as previously provided. The choice of the experimental procedure to be adopted must follow the desired structural characteristics, such as pore size, surface area, wall thickness, homogeneity, crystallinity, active sites, and surface properties of mesoparticles. As a result of this, some factors influence the synthesis of MCM-41 mesoparticles, such as: crystallization temperature, silica source, solution pH, co-solvent use, surfactant type, and surfactant/SiO_2 ratio. In addition, the removal process of template of internal structure of mesoparticles is an important variable in the synthesis of mesoporous materials. The use of calcination decreases the time to remove the template. On the other hand, this process can damage the ordered structure of mesoparticles [81]. The literature already presents alternative forms for this step in the synthesis, with milder temperatures or solvent extraction. However, they present as disadvantages more laborious procedures and require additional steps of drying for the total removal of solvents used in this process. In this way, the procedure to be adopted must meet the needs of the scientific work developed with an attempt to reduce additional steps and operational costs. Some of silicas and surfactants used in the literature for obtaining MCM-41 have been described below.

Amorphous silica is the wall-building unit of MCM-41-based mesoporous materials. Various silica sources can be used for the synthesis of mesoporous matrix, such as sodium silicate [98] and TEOS [95]. In addition, tetramethylorthosilicate (TMOS), sodium aluminate, aluminum sulfate, aluminum nitrate, metakaolin, and aluminum isopropoxide or silica are used as a silica and/or aluminum sources [84].

Mody et al. [99] presented the synthesis of MCM-41 mesoparticles with sodium silicate in less than 3 h using a simple methodology at room temperature. Cai et al. [68] reported the preparation of MCM-41 with suitable textural properties using TEOS. Whole Corma et al. [100] presented the preparation of MCM-41 with amorphous silica and tetramethyl ammonium silicate as silica sources. The mesoparticles produced were modified with Ti and applied in the selective oxidation catalysis of hydrocarbons. In addition to the commercial silicas, other alternative materials were employed as an inexpensive alternative source of amorphous silica to produce MCM-41-based mesoporous materials of technological interest. Wang et al. [101] presented a synthesis route of mesoporous material with regular mesopores, high surface area, and wall thickness consistent with MCM-41. For its production, TEOS and metakaolin were used as a silica and aluminum sources. Siriluk and Yuttapong [102] presented the synthesis of MCM-41 using silica extracted from the rice husk ash. The crystallinity, porosity, and surface area were similar with a material produced from commercial sodium silicate.

On the other hand, Sanhueza et al. [103] obtained MCM-41 mesoporous material using diatomite and pumicite as an alternative silica. Du et al. [104] used montmorillonite and kaolinite as a silica sources to produce MCM-41. The materials exhibited high surface areas and pore diameters compatible with MCM-41 synthetized with commercial silica. In addition, the materials were tested in the remediation of Pb(II) and the mesoporous materials presented satisfactory results for the Pb(II) removal from aqueous solutions. Jiang et al. [105] successfully synthesized the MCM-41 using inexpensive kaolin as partial silica source. The mesoporous material presented thermal and hydrothermal stability compatible with materials from commercial silicas. In addition, the material was tested as a catalyst and the results proved to be efficient. Differently, Lvov et al. [106] prepared a thermal and mechanical stable composite (MCM-41/halloysite) by the incorporation of ordered MCM-41 on halloysite, which showed good catalytic and adsorbent results.

The silica used to produce the MCM-41 may offer different properties for the mesoparticles. The use of commercial silicas, such as TEOS or TMOS, is relatively expensive, as well as, brings some disadvantages, such as high cost and toxic effect. Research with alternative sources can be an attractive alternative to reduce impacts on the environment and human health. To be a candidate for silica source, the material must have high silica content coupled with low cost and toxicity and eco-friendly. There is still much to be discussed and researched in the field to obtain sustainable and inexpensive silica sources with high efficiency in the sustainable development of new advanced multifunctional materials [107].

The surfactant that is used as a template to form the uniform porous structure is the key parameter that determines the shape of pores in the formation of amorphous silica structures. It is a molecule consisting of one hydrophilic and one hydrophobic part. According to the hydrophilic part, they can be classified as ionic and non-ionic. The anionics, in aqueous solution, have one or a few ionic groups producing negatively charged ions on the active surface. Yokoi and Tatsumi [108] reported that anionic surfactants are produced in large quantities, as well as being used in various applications because they have a relatively low cost. The cationics, in aqueous solution, have one or more ionizable groups that produce positively charged ions on the active surface. This is the class of surfactants most adopted by researchers. Wang et al. [109] presented the synthesis of MCM-41 mesoparticles with CTAB as template. The mesoporous material was produced near room temperature, but presented large pore volumes, specific surface areas, and typical hexagonal mesoporous structure of MCM-41. Amphoterals have in their structure acidic and basic radicals and in aqueous solutions they exhibit anionic or cationic characteristics, depending of the solution pH. Park et al. [110] reported that anionic surfactants are generally used in the preparation of MCM-41 mesoparticles, but few reports of mesoporous synthesis with amphoteric templates. The researchers successfully produced mesoporous materials with hexagonal ordered structure with an amphoteric surfactant of amino acid type [111].

Léonard et al. [112] presented the synthesis of mesoporous materials with the non-ionic deacoxyethylene cetyl ether directing agent [$C_{16}(EO)_{10}$]. The materials synthesized presented ordered structures at intermediate pH values, as the medium affects the silica hydrolysis, condensation rates, and surfactant-silica interactions. Whole Chen et al. [113] reported the use of two types of surfactants [CTAB (cationic) and sodium laurate (anionic)] in order to facilitate the formation of mesoparticles and to be considered a low-cost method. On the other hand, recently, our research group synthesized the MCM-41 mesoporous material by using hydrothermal method in the presence of 1-butyl-2,3-dimethylimidazolium hexafluorophosphate ([BMMIM]PF_6) ionic liquid (IL) as template [51].

The pore size of MCM-41 mesoporous material can be controlled by the size of the hydrophilic chain of surfactant or with the use of auxiliary organic compounds termed spacers. When these compounds are added to the synthesis gel, they solubilize into the micelles by the hydrophobic region causing an increase in the micelle diameter. Therefore, the increase of the pore diameter of material is achieved [114]. Another parameter that can be altered by the choice of surfactant is the pore wall thickness. The use of ionic surfactants causes strong electrostatic attraction between the template and the inorganic species resulting in a thicker-walled material. The pH of medium has little influence on this parameter. In addition, primary amines, with 8–18 carbons, were employed by Tanev and Pinnavaia [115] to increase the pore wall thickness providing greater thermal and hydrothermal stability. Wei et al. [116] proposed the synthesis of MCM-41 mesoparticles with small organic molecules. In similar systems, the pore diameter is defined by the concentration of organic molecules. The template removal can be performed by washing, solvent extraction or calcination. The advantage of this method is the easiness of template removal, as well as low cost of process [117].

3. Methods of functionalization of mesoporous material

The surface modification of MCM-41-based mesoporous materials can be performed via functionalization of mesoparticles with inorganic or organic groups on the surface of mesoporous matrix. Properties such

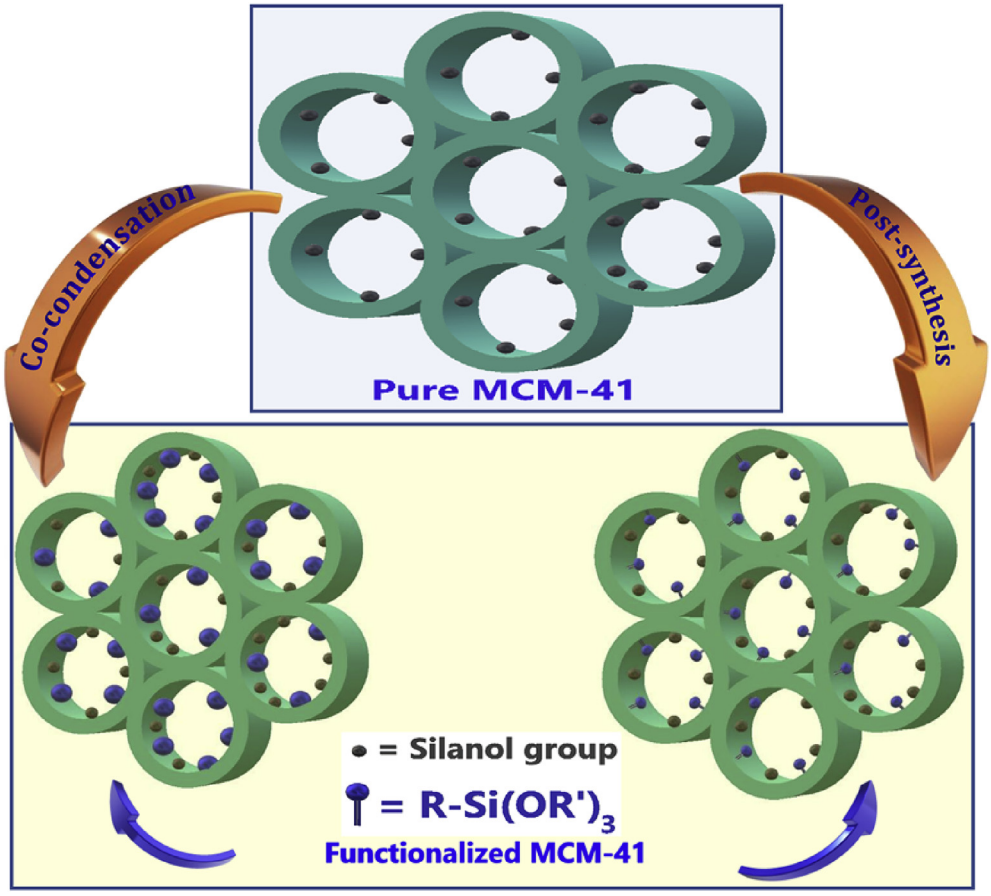

Fig. 4. Methods of superficial modification of MCM-41 mesoporous material.

as hydrophilicity, hydrophobicity, acidity, basicity, and binding to guest can be promptly achieved and the modification of the bulk properties of mesoparticles, while at the same time, stabilizing the materials towards hydrolysis. The framework of MCM-41 mesoparticles have SiO_2 tetrahedra terminating in either siloxane (Si–O–Si) or silanol (Si–OH) groups on the surface. Both groups are reactive for functionalization, although the reaction with silanol groups is considered the main route of modification, since they provide unique anchoring sites for the functionalization of species within the pores of mesoparticles [118]. There are two strategies for the superficial functionalization of mesoporous matrix: **(i)** post-synthesis and **(ii)** co-condensation methods. Fig. 4 shows the different mechanisms of superficial modification of mesoporous materials.

3.1. Co-condensation

This method of superficial modification was proposed by Mann and collaborators [119]. In this one-pot synthetic method, the silica source and the functionalizing agent, such as metal ions or organosilane species, are added slowly in the reaction medium at the same time or in sequence so that they undergo hydrolysis and condense in around the structure directing micelles. Thus, the functionalizing agent can be incorporated homogeneously into the outer walls, as well as the internal structure of the mesopores of mesoporous matrix, resulting in the control of morphology of functionalized mesoparticles [120–122]. For example, Lee et al. [123] prepared the Mn-MCM-41 and Zr–Mn-MCM-41 mesoporous materials using a direct mixture of Mn [manganese (II) acetate] and Zr [zirconium (IV) isopropoxide] sources with the silica, Carrott et al. [73] used a mixture of tetraethoxysilane, titanium ethoxide in propan-2-ol, hexa- or octadecyltrimethylammonium bromide, and ammonia for the direct synthesis of Ti-MCM-41, while Bengueddach et al. [124] using a mixture of sodium aluminate and TEOS (Al and Si sources, respectively) in basic medium prepared Al-MCM-41 mesoporous material. Thus, all mesoporous materials showed high surface area and pore volume values, well-defined mesoporous structures, and thermal stability.

The stability of MCM-41 functionalized mesoparticles can be affected by the presence of defects in the structure matrix. These defects come from the metal ion or organosilane inside the walls. This limits the concentration of these modifiers on the surface because the higher the concentration more unstable the structure becomes. In addition, another disadvantage of this method is the subsequent surfactant removal through calcination. At elevated temperatures the destruction of covalently bound modifying functionality occurs. Therefore, the template removal could be performed using the solvent extraction in reflux.

3.2. Post-synthesis

The post-synthesis methods are various, such as: **(i)** impregnation, **(ii)** ionic exchange of surfactant, and **(iii)** immobilization, among others [122]. In the wet impregnation method, the volume of solvent added to MCM-41 is equal to its pore volume. While in the impregnation by evaporation, the amount of solvent added exceeds the pore volume of MCM-41 [125,126]. In the indirect ion exchange method, during the synthesis of MCM-41 mesoparticles with cationic surfactant, the hydrophobic region of conductor, which has a positive charge, interacts with the pore surface of the mesoporous material through coulombic interaction. During the ion exchange process this interaction is broken and the cationic surfactant is replaced by a metal cation [122].

The immobilization method is commonly employed because of its synthetic simplicity and flexibility in the introduction of surface groups, which is done after surfactant removal. A primary aspect is the

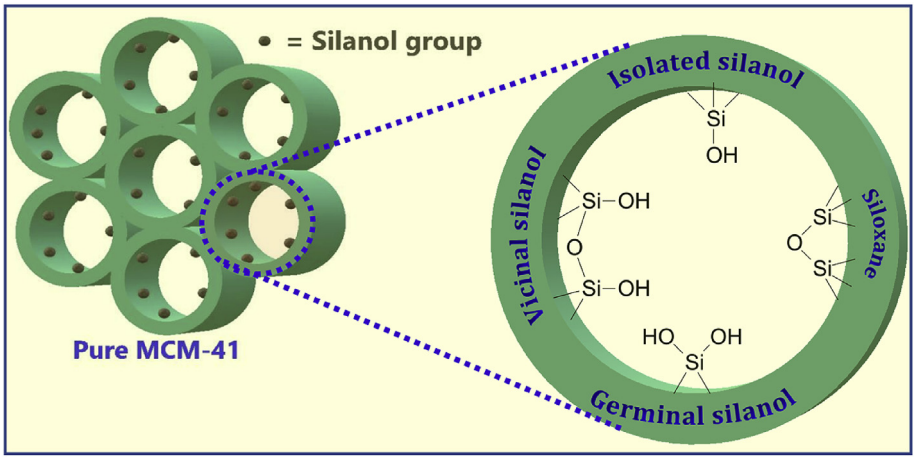

Fig. 5. Types of silanol groups on the surface of MCM-41 mesoparticles.

calcination process for the surfactant removal, which affects the density of surface silane groups on the MCM-41 matrix [75]. There are four types of silanol groups on the surface of MCM-41 mesoparticles: **(i)** terminal silanol groups (isolated or free silanol), **(ii)** geminal silanol groups, **(iii)** ethereal silanol groups (siloxane), and **(iv)** vicinal silanol groups (hydrogen-bonded) (Fig. 5) [127]. Zhao and collaborators reported that the density of terminal, geminal, and vicinal silanol groups on a mold extracted MCM-41 is about 3.0 per nm^2 [75].

The silanol groups are the active sites for the anchoring organic groups on the surface of mesoporous array. Ideally, an intermediate temperature for calcination (e.g., 350–550 °C) is required for there to be a higher concentration of silane groups. At lower temperatures, a large number of silanol groups are not available for covalent anchoring due to hydrogen bonding and/or physically adsorbed water; finally, at high temperatures the silanols are lost due to condensation reactions [128].

Superficial functionalization with organic groups after calcination is usually carried out by direct reaction of organosilanes with the silane groups. The advantages of this method are: the final structure of mesoparticles after the functionalization remains orderly, the resulting material presents high hydrothermal stability and the functional groups can be chosen according to the predetermined objectives [129]. For functionalization of mesopores, alkoxysilanes or chlorosilanes having short carbon chains as the spacer and functional end groups are generally used, such as amino, mercapto, and vinyl).

Studies with MCM-41-based functionalized mesoporous materials have presented a greater number of researches due to the variety of applications, especially in the area of adsorption. Modified mesoporous materials with organic groups are susceptible to higher adsorption of negatively charged dyes [37]. Park and collaborator reported that peak H_2 consumption of MCM-41 modified with Ni was 0.68% [130]. Therefore, the Brønsted acidity plays an important role in the adsorption studies of H_2 when compared to pure material. MCM-41 mesoparticles modified with mercaptan groups are important in the adsorption of heavy metals in environmental matrices. Different techniques are used to characterize the MCM-41 functionalized mesoporous material, such as N_2 adsorption and desorption, XRD, TEM, solid state NMR, FTIR, thermogravimetric analysis (TGA), X-ray photoelectron spectroscopy (XPS), among others. Table 1 summarizes the various functionalization methods, modifier groups, and the application of MCM-41-based mesoporous materials in recent years (2010–2019).

4. Applications of MCM-41-based mesoporous material

The MCM-41 mesoporous material, as well as the functionalized MCM-41 with different groups has been applied in most different applications in the literature. Based on this, Fadhli et al. [174] used the Ti/MCM-41 catalyst for enantioselective epoxidation of styrene. MCM-41 modified with Al (Al-MCM-41) is widely used as catalytic support because the Al-MCM-41 allows the diffusion and adsorption of large molecules (substrate and/or reaction products), such as polycyclic aromatic hydrocarbons, volatile organic compounds, and sulfur substances, due to its textural and structural properties [175–177]. Therefore, Karakhanov et al. [177] used the Al-MCM-41 support in the hydroconversion of 1-methylnaphtalene (1 MN), 2- methylnaphthalene (2 MN), and dibenzothiophene (DBT) compounds, and Vinokurov et al. [176] prepared the Al-MCM-41 support impregnated with lanthanum for the catalytic cracking of sulfur organic compounds.

On the other hand, Khan et al. [147] prepared the mixed matrix membrane (MMM) of the polysulfone acrylate with MCM-41-NH_2 for the CO_2 separation, and Qi et al. [46] used the MCM-41/polypyrrole hybrid film as humidity sensor. While, Patrushev and Sidelnikov [178] used the organic-inorganic MCM-41 as stationary phase for the separation of C_1–C_4 hydrocarbons on the capillary columns, Jesus et al. [48] applied the MCM-41 in the efavirenz release system, and Li et al. [179] used the MCM-41 nanospheres on graphene oxide as fire retardant in the epoxy resin. Ulu et al. [163] prepared the epoxy-modified Fe_3O_4@MCM-41 as support for L-ASNase enzyme, Woszuk et al. [180] used the MCM-41 as additive for warm mix asphalts, and Mortera et al. [181] prepared the bioactive glass-ceramic scaffold from MCM-41.

As explained above, it is possible to observe that the MCM-41 has been used in the most varied technological applications and this is only possible due to its textural and structural properties already mentioned in the present work. Recently our research group used pure MCM-41 as sorbent in matrix solid phase dispersion (MSPD) method for the determination of pesticides in soursop fruit (*Annona muricata*) [36], as well as evaluated the photoluminescent properties of the functionalized Ln-PABA-MCM-41 [170]. However, the focus of our group has been the development of the multifunctional mesoporous materials to be applied in the adsorption technology of organic and inorganic compounds. Therefore, this work was directed in a review of use of the MCM-41 mesoporous material as adsorbent material for the removal of organic and inorganic compounds.

4.1. Adsorption technology

In the literature there are several methods used for the remediation/removal of organic and inorganic compounds, such as biotransformation in biological system [182], photolysis [183], filtration and/or ultrafiltration [184–186], biofiltration [187,188], reverse osmosis [189,190], oxidation and/or coagulation [45,191,192], dielectric barrier discharge reactor [193], fuel cells [194], ion exchange [195,196], electrokinetics [197,198], electrodialysis [199], photocatalysis [200],

Table 1
Functionalization methods, modifier groups, and the different applications of MCM-41-based mesoporous materials in recent years.

Functionalization method	Modified group	Application	Reference
Wet Impregnation	Amine	CO_2 adsorption	[131]
Immobilization	Para-phenylamino sulfonic acid	Catalytic	[132]
Wet Impregnation	Polyethylenimine	CO_2 adsorption	[121]
Wet Impregnation	Tetraethylenenpentamine	CO_2 adsorption	[133]
Immobilization	(3-Chloropropyl)triethoxysilane	Catalytic	[134]
Immobilization	Amine and carboxyl	Drug delivery	[135]
Immobilization and impregnation	Quercetin	Topical application	[136]
Immobilization	Chloro(dimethyl)vinylsilane and trimethoxy(7-octen-1-yl)silane	Catalytic	[137]
Immobilization	3-Aminopropyltriethoxysilane	Drug delivery	[138]
Immobilization	3-Aminopropyltriethoxysilane	Cr(VI) adsorption	[139]
Immobilization	Chitosan	Pb(II) adsorption	[140]
Immobilization	(Methylmercapto)undecyltrimethoxysilane	Catalytic	[141]
Immobilization	N-[3-(trimethoxysilyl)propyl]-ethylenediamine	Catalytic	[142]
Immobilization	3-Mercaptopropyltriethoxysilane	Catalytic	[143]
Immobilization	3-Mercaptopropyltrimethoxy-silane and N-(3-trimethoxysilylpropyl)diethylenetriamine	Hg^{2+} adsorption	[144]
Immobilization	3-Mercaptopropyltrimethoxysilane	Gas separation	[145]
Immobilization	Trimethoxysilylpropylamine	Drug delivery	[146]
Immobilization	Aminopropyltrimethoxysilane	CO_2 separation	[147]
Immobilization	3-Aminopropyltrimethoxysilane, 3-(N, N-dimethylaminopropyl)triethoxysilane and 3-trimethoxysilylpropylethylenediamine	Catalytic	[148]
Co-condensation	3-[2-(2-Aminoethylamino)ethylamino]propyl trimethoxysilane	Nitrate removal	[149]
Co-condensation	Meta-aminobenzoic acid	Optical or electronic	[150]
Immobilization	Amino groups and phosphotungstic acid	Catalytic	[151]
Immobilization	3-Aminopropyltriethoxysilane and triethoxysilanevinyl	Drug delivery	[152]
Immobilization	(3-Aminopropyl)triethoxysilane	Dye adsorption	[153]
Immobilization	3-Mercaptopropyltrimethoxysilane	Catalytic	[154]
Immobilization	Pentane-1,2-dicarboxylic acid	Fe^{3+} adsorption	[155]
Immobilization	(3-Chloropropyl)trimethoxysilane	Catalytic	[156]
Co-condensation, wet impregnation, and immobilization	Hydroquinone	Catalytic	[157]
Immobilization	3-Aminopropyltriethoxysilane	Dye removal	[158]
Immobilization	$(Pb(NO_3)_2$, $Zn(NO_3)_2{\cdot}4H_2O$ and $(Ni(NO_3)_2{\cdot}6H_2O)$	Adsorption	[159]
Immobilization and impregnation	Amino	CO_2 adsorption	[160]
Co-condensation	Sulfonic acid	Catalytic	[161]
Wet impregnation	12-Tungstophosphoric acid	Drug delivery	[162]
Immobilization	3-Aminopropyltriethoxysilane	Cd(II) removal	[127]
Immobilization	L-Asparaginase	Catalytic	[163]
Impregnation	Polyethylenimine	Gas Separation	[164]
Immobilization	3-Aminopropyltriethoxysilane	Catalytic	[165]
Immobilization	3-Aminopropyltriethoxysilane	Catalytic	[166]
Immobilization	3-(2-Cyanoethylsulfanyl)propyltriethoxysilane	Catalytic	[167]
Immobilization	(3-Mercaptopropyl)trimethoxysilane	Catalytic	[168]
Co-condensation	Tungsten	Catalytic	[169]
Immobilization	3-Aminopropropyltrimethoxysilane	Dye adsorption	[37]
Co-condensation and immobilization	p-Aminobenzoic acid	Photoluminescence	[170]
Co-condensation	p-Aminobenzoic acid	Solid phase extraction	[171]
Co-condensation	Manganese Zirconium–Manganese	–	[123]
Co-condensation	Aluminum	Dye adsorption	[124]
Co-condensation	Titanium	–	[73]
Co-condensation	Zirconium	Catalytic	[172]
Co-condensation	Titanium–Germanium	Catalytic	[173]

bioremediation [201,202], phytoremediation [203,204], and other. However, the adsorption technology is one of the most used for the removal of pollutants from different pollution sources. This wide use of the adsorption process, in detriment of the other remediation techniques cited, is due to the fact that this is a versatile method, economical, efficient, low-cost, easy to use, eco-friendly, does not generate waste or by-products, as well as allows the reuse of adsorbent and adsorbate after the removal process [37,38]. Thus, in the present review, we cover the main uses of MCM-41-based mesoporous material in the remediation processes of organic and inorganic compounds, as well as gas molecules by adsorption mechanism.

4.1.1. Factors that affect the adsorption process

The adsorption process can be influenced by different factors, either alone or in a combination of these factors. Among the factors most studied in the adsorption processes we can highlight: **(i) Solution pH**: the adsorbents can present different ionic species in a wide range of pH values, as well as the surface of adsorbent mesoporous material can undergo alteration of surface charge from the pH variation of system. In this way, the adsorptive process can be governed directly by an electrostatic interaction mechanism between the adsorbent material and adsorbate; **(ii) Initial concentration of adsorbate**: the number of adsorbate molecules may have a positive effect on the adsorption efficiency of an adsorbent material. This behavior can be explained by adsorption process occurring mainly at the outermost active sites of mesoporous material surface when the initial adsorbate concentration was low, with migration towards sites deeper within the mesoporous material at higher initial adsorbate concentrations. This behavior was observed by some work of our research group in the removal of organic compounds [37,38,86,87]. Moreover, it is possible to obtain relevant information about the maximum adsorption efficiency of an adsorbent material, as well as to make a more in-depth interpretation of the theoretical models of adsorption isotherms [38,86,87]; **(iii) Adsorbent amount**: the adsorbent material amount is an important parameter that

can directly influence in the removal efficiency of a adsorbent during the removal process of the different adsorbates. The increase in the adsorption efficiency can be attributed to the increased availability of active sites from the adsorbent material that can be used for adsorption of molecules during the process [37]; **(iv) Contact time**: the variation of contact time is an important parameter to be evaluated in the adsorption process, since from this study it is possible to obtain information of initial rate until adsorption equilibrium of process, as well as to do a more in-depth study of the theoretical models of adsorption kinetics [37,38,86,87]; **(v) Temperature**: the temperature is a very important parameter in an adsorption process in order to obtain information about the kinetic energy, mobility, solubility, and chemical potential of adsorbate molecules during the adsorption process, as well as to obtain valuable information about the thermodynamic parameters that govern the adsorption mechanism, mainly Gibbs energy (ΔG), enthalpy (ΔH), and entropy (ΔS) [37,86,87]. However, some works of group have shown that the removal efficiency of PAHs by the MCM-41 and PABA-MCM-41 mesoporous materials is not influenced by the variation of adsorption temperature [86,87].

4.2. Use of MCM-41-based mesoporous materials in adsorption process

4.2.1. Organic compounds

It is not today that researchers are concerned about environmental contamination with organic compounds, because many of these compounds are classified by Environmental Agencies as toxic, allergenic, pathogenic, carcinogenic, mutagenic, recalcitrant, non-biodegradable, teratogenetic, as well as in many cases, they act as endocrine disruptors or affect the hormonal control [37,38,86,87,205–207]. Therefore, these organic compounds can pose a danger to the living beings in general and can generate human health problems, as well as for ecosystems, because in many cases the wastes containing these compounds are improperly disposed or without due treatment.

In this way, these organic compounds come from different sources of pollution, such as discharges, petroleum spills, combustion of fossil fuels, automobile exhaust emissions, and nonpoint sources such as urban runoff, in the case of polycyclic aromatic hydrocarbons (PAHs) and volatile organic compounds (VOCs). Our research group has been developing some functionalized mesoporous materials from the functionalization of pure MCM-41 to be used in the removal of PAHs, for example, the Si-MCM-41 presented a removal efficiency of 90.40, 90.84, and 92.98% in the remediation of benzo[k]fluoranthene, benzo [b]fluoranthene, and benzo[a]pyrene, respectively [38], in only 60 min of adsorption at 25 °C. In turn, PABA-MCM-41 functionalized mesoporous material presented, at 25.0, 35.0, and 45.0 °C, the removal percentage of 96.2, 96.3, and 96.4%, respectively, for the benzo[a] pyrene in 90 min until to equilibrium [86]. In this case, no significant differences were observed with the temperature increasing. Also, the pure MCM-41 presented the q_e values of 12.49 and 18.06 μg g^{-1} in the removal of benzo[k]fluoranthene and benzo[b]fluoranthene, respectively. However the q_e values of 22.51 and 26.58 μg g^{-1} were found for the functionalized MCM-41 (PABA-MCM-41) [87].

Araújo et al. [208] found q_m values of 0.69, 0.54, and 0.34 mmol g^{-1} at a temperature of 25, 40, and 60 °C, respectively, in the naphthalene removal, as well as 1.26 (25 °C), 1.01 (40 °C), and 0.67 mmol g^{-1} (60 °C) for anthracene, and 1.31 (25 °C), 1.09 (40 °C), and 0.76 mmol g^{-1} (60 °C) for the pyrene removal by MCM-41. According to the authors, these results should be an exothermic nature of interaction of PAHs with mesoporous material, because the q_m values obtained in the process decrease with increasing of adsorption temperature. In turn, Hu et al. [209] used the MCM-41-dry for the phenanthrene removal and obtained removal efficiency of 94% with an adsorbent amount until to 0.4 g L^{-1}. In this work, they showed that pH variation was insignificant. Some studies show the removal of aromatic organic compounds in wastewater or laboratory scale. For example, Yang et al. [210] obtained an aniline removal by C-MCM-41-3 of 94.52% at pH 1 with 4 g L^{-1} of adsorbent amount in 2 h. However, only 0.71% at pH 13. In this work it was possible to observe that the pH variation directly influenced the adsorption efficiency of mesoporous material, as well as Toor et al. [211] obtained 64.73% of removal of 4-aminobiphenyl by MCM-41 at pH 2. However, the MCM-41 presented an irrelevant efficiency at pH values between 6 and 9, due to changes in the surface charges of mesoporous material and 4-aminobiphenyl at different pH values. On the other hand, Sadeghi et al. [159] were able to remove more that 90% of chloroethyl phenyl sulfide (CEPS) using the Pb-MCM-41/$ZnNiO_2$ mesoporous nanocomposite adsorbent. They observed an increase in the adsorbent material efficiency with increasing of dose and time of adsorption, but the efficiency decreased with increasing CEPS concentration.

Some works also report the removal of organic compounds from of tanning and textile industries (e.g., dyes, ethylenediaminetetraacetic acid), as well as nuclear power plant (e.g., oxalic acid, picric acid). In this sense, our research group tested the adsorption efficiency of functionalized mesoporous material (NH_2-MCM-41) in the removal of remazol red dye and found a maximum adsorption efficiency of 99.1% (q_e = 45 mg g^{-1}). We also observed that the adsorption capacity of functionalized mesoporous material increased with adsorption time, NH_2-MCM-41 amount, temperature, and dye concentration, but decreased when the solution pH was higher [37]. The same behavior was observed by Zhou et al. [212] in the removal of methylene blue by Al-MCM-41. However, in this case, the adsorption capacity increased with increase of solution pH and decreased at high temperature. Thus, the maximum adsorption capacity values (q_m) found at temperatures of 298, 308, and 318 K were 277.78, 276.24, and 272.48 mg g^{-1}, respectively, at pH 10. Wu et al. [213] obtained maximum adsorption capacity of 140.60 mg g^{-1} (25 °C), 134.78 mg g^{-1} (30 °C), and 133.33 mg g^{-1} (40 °C) for fuchsine (pH 2) and 278.38 mg g^{-1} (25 °C), 224.54 mg g^{-1} (30 °C), and 203.56 mg g^{-1} (40 °C) for acid orange II (pH 3) in the remediation by NH_2-MCM-41. However, it was observed in this work that the adsorption capacity decreased with increasing NH_2-MCM-41 amount. On the other hand, Shu et al. [214] achieved a maximum adsorption efficiency of methyl blue of 121.34, 157.48, 181.82, and 189.04 mg g^{-1} at 15, 25, 50, and 80 °C, respectively, employing 20 mg of Ni-MCM-41 at pH 6.32.

Ethylenediaminetetraacetic acid (EDTA) and oxalic acid are widely used industrially as a chelating agent. However, the presence of these compounds in wastewater may present serious environmental problems. Gokulakrishnan et al. [215] used the Al-MCM-41 for the EDTA removal. The authors obtained a removal efficiency of EDTA of 89.8% in 150 min of adsorption with Al-MCM-41 (Si/Al = 25). The same author [216] obtained adsorption capacity values of oxalic acid with Al-MCM-41 (Si/Al = 25) of 58.5, 45.6, 36.3, 28.6, 22.7, 19.0, and 16.7 mg g^{-1} at pH 1, 3, 5, 7, 9, 11, and 13, respectively. Another toxic organic compound from explosives and textile factories that makes it difficult to reuse wastewater is picric acid [217]. Sepehrian et al. [217] obtained more than 82% of picric acid removal at an initial time of 2 min with the UC-MCM-41 adsorbent. In this work, it is possible to observe that the pH increases from 4 to 5 and 6 caused a decrease in the removal efficiency of picric acid by UC-MCM-41 adsorbent.

Pharmaceutical and personal care products (PPCPs) are other sources of organic compounds that can cause contamination, even in low concentration, in fresh water intended for human consumption, as well as to aquatic organisms. These drugs are water soluble and are not completely absorbed by human metabolism and thus being able to reach water bodies in various ways [205]. Therefore, numerous studies have been carried out in the application of mesoporous materials for the removal of these compounds. Akpotu and Moodley [205] used the ASM41 (as-synthesized MCM-41), MCM-41-GO, and MCM-41-G mesoporous materials for removal of acetaminophen and aspirin, and it was found experimental q_e values of 1.81, 6.46, and 10.9 mg g^{-1} for the acetaminophen and of 33.0, 8.11, and 9.68 mg g^{-1} for the aspirin, respectively, for the ASM41, MCM-41-GO, and MCM-41-G mesoporous

materials. It is also possible to observe that pH alteration had little influence on the acetaminophen adsorption by ASM41, MCM-41-GO, and MCM-41-G, as well as in the aspirin removal by ASM41 and MCM-41-GO. However, the adsorption efficiency of MCM-41-G decreased with increasing pH from 2 to 10. Chen et al. [206] obtained the maximum adsorption capacity for the norfloxacin by Fe-MCM-41 of 134.26, 102.90, and 109.34 mg g^{-1} in the temperature of 288, 298, and 308 K, respectively, in approximately 30 min of adsorption at an optimum pH of 7. Gao et al. [218] used the Pr-MCM-41 for the adsorption of estrone (E1), 17β-estradiol (E2), and 17α-ethinyl estradiol (EE2) and the mesoporous material presented the maximum adsorption capacity of 88.38, 86.91, and 119.87 mg g^{-1} in the removal of E1, E2, and EE2, respectively, with the equilibrium time of adsorption of approximately 20 min, pH 7, and temperature of 25 °C.

Guo et al. [219] obtained a maximum adsorption capacity of 526.3 mg g^{-1} in the tetracycline removal by Fe-MCM-41-A, in 1 h of adsorption (pH 5 at 25 °C), while Liu et al. [220] found a value of 419 mg g^{-1} in the removal of the same compound by A-MCM-41 (optimum pH 3 and 323 K). On the other hand, Hossain et al. [221] obtained a removal capacity of urease of 102 mg g^{-1} (pH 7.2) with PE-MCM-41. Katiyar et al. [222] showed a removal efficiency of more than 150 mg g^{1} of bovine serum albumin (pH 5) and of 255 mg g^{-1} of lysozyme (pH 7.6) using the MCM-41, while Sun et al. [223] achieved maximum adsorption capacities of DNA of 44.7, 42.7, and 36.7 mg g^{-1} for the Al^{3+}-MCM-41, La^{3+}-MCM-41, and Zn^{2+}-MCM-41, respectively.

The indiscriminate use of agrochemicals in agricultural from various crops has significantly increased the contamination of environment with these highly toxic compounds. On the face of it, some research is being carried out with the objective of improving the removal process of these compounds of environment from the adsorption technology. Tian et al. [224] used the MCM-41 for the removal of 1,1,1-trichloro-2,2́ bis(*p*-chlorophenyl)ethane (DDT) and obtained a removal efficiency of ~92% after 36 h of adsorption using 50 mg of the adsorbent. Brigante and Avena [225] observed that the adsorption of dicationic herbicide paraquat (PQ^{2+}) by MCM-41 SiO_2 increase as pH increases and with temperature decrease. Thus, the maximum adsorption capacity was 416 μmol g^{-1}.

Another environmental problem is the processes of treatment and disinfection of water, because in some of these processes can lead to the generation of disinfection byproducts by reactions with natural organic matter (aquatic humic substances) present in the water bodies [226,227], as well as the high level this byproducts in aquatic environments can be caused serious public health problems [228]. Therefore, Ebrahimi-Gatkash et al. (2017) used the amino-functionalized mesoporous MCM-41 silica to remove nitrate anion and obtained maximum adsorption capacity of 31.7, 38.6, and 38.8 mg g^{-1} in the nitrate removal by N-MCM-41, NN-MCM-41, and NNN-MCM-41 mesoporous materials, respectively, in 2 h of adsorption at a temperature of 25 °C and pH 7. While Li et al. [229] achieved q_m values of 64.2, 51.9, and 46.2 mg g^{-1} in the phosphate removal by MCM-41-CFA-10 in the temperatures of 298, 308, and 318 K, with equilibrium time close to 50 min and 5 mg of mesoporous material. On the other hand, Seliem et al. [230] obtained a removal of only 21.01 mg g^{-1} of phosphate by composite of MCM-41 silica with rice husk at optimum values of pH 6 and dose = 200 mg. Table 2 catalogues the variety of MCM-41-based mesoporous materials that have been investigated for the removal of various organic compounds.

4.2.2. Inorganic compounds

The rampant industrial development, as well as the dynamics of population growth, have considerably elevated environmental contamination with toxic metals considered, as many of these are classified as bioaccumulation, non-biodegradability, toxic at very low concentration, persistent, and carcinogenic [248–250]. These metals can come from most different forms of pollution, mainly automotive [251], galvanic [252], electrical [250], fuel [249], dye and pigment [253], metallurgy [254], leather [255], nuclear industries [256], and other.

In view of these characteristics, the undue disposal of these metals can be a constant threat to environment and humans. In this way, many studies have shown the application of MCM-41 as adsorbent material for the removal of heavy metal. Boojari et al. [254] obtained q_m values of 133.3 and 102.1 mg g^{-1} in the As(III) and As(V) removal by α-Fe_2O_3/MCM-41, respectively, at a temperature of 298 K and equilibrium time of approximately 240 min. It is also possible to observe that the increase in the temperature has shown a reduction in the adsorption efficiency of α-Fe_2O_3/MCM-41 for the two metal species, but the increase in pH had a negative influence in the As(V) adsorption, whereas pH 7 was ideal for the As(III) removal. Benhamou et al. [255] used of MCM-41 for the Cr(VI) and As(V) removal, whose q_m values obtained in the pH 3.1 were of 25.2 and 18.0 mg g^{-1} in the Cr(VI) and As(V) removal. While that Chen et al. [257] reached a maximum adsorption capacity of 147 and 156 mg g^{-1} in the simultaneous removal of Pb^{2+} and MnO_4^-, respectively, using NH_2/MCM-41/NTAA at a pH value of 5.0 for Pb^{2+} and 3.0 for MnO_4^- and equilibrium time of approximately 40 min for both species and El-Naggar et al. [258] obtained removal efficiency of 99.9, 79.0, and 48.8% for the Pb^{2+} removal, 87.42, 69.15, and 42.70% for Cu^{2+}, and only 3.52, 2.78, and 1.72% for the Cd^{2+} remediation by MP/MCM-41 composite for the specie concentrations of 10, 100, and 250 mg L^{-1}, respectively.

Following this reasoning, Yilmaz et al. [43] performed the Sr^{2+} removal with MCM-41 mesoporous material and obtained value of q_m = 9.97 mg g^{-1}. Javadian and Taghavi [259] obtained 163.93 mg g^{-1} of Hg^{2+} removal by MCM-41 nanocomposite, Fu et al. [260] presented a value of q_m = 179.43 mg g^{-1} also in the Hg^{2+} removal by a functional hybrid mesoporous composite material, and Eanche et al. [261] removed 129.87 and 138.88 mg g^{-1} of Pb(II) with MCM-41 and MCM-41@salen mesoparticles, respectively. The use of mesoporous materials for the removal of radioactive species is also reported in the literature. Sert and Eral [256] reported a maximum adsorption capacity of uranium of 625 mg g^{-1} by NH_2-MCM-41, while Sepehrian et al. [262] presented a value of only 18.08 mg g^{-1} using pure MCM-41 mesoporous material. On the other hand, Guo et al. [263] showed that the MCM-41and MCM-41-SH have a maximum adsorption of 15 and 30 mg g^{-1} of Cs removal, respectively. Table 3 shows some MCM-41-based mesoporous materials that were used for the remediation of various inorganic compounds.

4.2.3. Gases

One of the main problems related to the emission of gases in the atmosphere can be said to be the release of greenhouse gases, which can contribute significantly to the increase of global warming. Of the so-called greenhouse gases, we can highlight the carbon dioxide (CO_2), which comes mainly from the combustion of fossil fuels [131,133]. The increase in the atmospheric pollution can also be caused by the emission of other gases, such as BTEX (benzene, toluene, ethylbenzene, and xylene), which can also cause serious problems for humans and environmental [284]; SO_x gases, which are responsible for acid rain [285]; gaseous polycyclic aromatic hydrocarbons (PAHs), these compounds are highly toxic, carcinogenic, and/or mutagenic [286], among others.

In view of the above problems, it is possible to observe that in the literature there are several works devoted to the study of gas removal and/or storage from the use of materials with mesoporous array. Zhou et al. [287] found adsorption capacity of CO_2 of 4.08 mmol g^{-1} (100 kPa and 298 K) using the 5A-MCM-41 composite, Wang et al. [288] obtained, receptively, adsorption efficiency of 2.45 and 3.50 mmol g^{-1} (15 vol% CO_2, 70 °C) using MCM-41-TEPA60% and MCM-41-APTS30%-TEPA40% mesoporous materials, Tari et al. [289] using the MCM-41 and MCM-41/Cu(BDC) composite for the removal of CO_2 and CH_4 with adsorptive amount values found of 14.2 and 14.15 mmol g^{-1} (MCM-41) and of 40.82 and 36 mmol g^{-1} [MCM-41/Cu (BDC)], respectively, at 303 K. While Sanz et al. [160] removed 16.1,

Table 2
Adsorption of various organic compound by mesoporous materials.

Material	Compound	pH	Temperature	Adsorption capacity	Efficiency (%)	Reference
Si-MCM-41	Benzo[k]fluoranthene	-	25 °C	18.26 μg g^{-1}	90.40	[38]
	Benzo[b]fluoranthene			18.35 μg g^{-1}	90.84	
	Benzo[a]pyrene			18.78 μg g^{-1}	92.98	
PABA-MCM-41	Benzo[a]pyrene	-	25 °C	27.2 μg g^{-1}	96.2	[86]
			35 °C	27.3 μg g^{-1}	96.3	
			45 °C	27.4 μg g^{-1}	96.4	
MCM-41	Benzo[k]fluoranthene	-	25 °C	12.49 μg g^{-1}	-	[87]
	Benzo[b]fluoranthene			18.06 μg g^{-1}		
PABA-MCM-41	Benzo[k]fluoranthene	-	25 °C	22.51 μg g^{-1}	-	[87]
	Benzo[b]fluoranthene			26.58 μg g^{-1}		
PABA-MCM-41 (RHA)	Naphthalene	5.6	25 °C	17.83 μg g^{-1}	89.08	[231]
	Benzo[b]fluoranthene			19.56 μg g^{-1}	97.80	
	Benzo[k]fluoranthene			18.91 μg g^{-1}	94.54	
	Benzo[a]pyrene			18.77 μg g^{-1}	93.85	
MCM-41 (RHA)	Naphthalene	5.6	25 °C	15.99 μg g^{-1}	79.94	[232]
	Benzo[b]fluoranthene			19.65 μg g^{-1}	94.34	
	Benzo[k]fluoranthene			19.06 μg g^{-1}	95.32	
	Benzo[a]pyrene			18.87 μg g^{-1}	98.25	
	Naphthalene		25 °C	0.69 mmol g^{-1}		
			40 °C	0.54 mmol g^{-1}		
			60 °C	0.34 mmol g^{-1}		
MCM-41	Anthracene	-	25 °C	1.26 mmol g^{-1}	-	[208]
			40 °C	1.01 mmol g^{-1}		
			60 °C	0.67 mmol g^{-1}		
	Pyrene		25 °C	1.31 mmol g^{-1}		
			40 °C	1.09 mmol g^{-1}		
			60 °C	0.76 mmol g^{-1}		
MCM-41-dry	Phenanthrene	6.45	15 °C	2266.5 μg g^{-1}	94	[209]
MCM-41-d	Bisphenol A	–	15 °C	416.7 μg g^{-1}	–	[233]
			25 °C	414.9 μg g^{-1}		
			35 °C	387.6 μg g^{-1}		
C-MCM-41-3	Aniline	7	298 K	16.64 mg g^{-1}	-	[210]
			308 K	15.69 mg g^{-1}		
			318 K	14.50 mg g^{-1}		
			328 K	13.68 mg g^{-1}		
MCM-41	Quinoline	–	–	–	68.22	[234]
Co-MCM-41					65.91	
MCM-41	4-Aminobiphenyl	2	303 K	-	64.73	[211]
Pb-MCM-41/$ZnNiO_2$	Chloroethyl phenyl sulfide	-	-	-	> 90	[159]
NH_2-MCM-41	Remazol red	2	55 °C	45 mg g^{-1}	99.1	[37]
Al-MCM-41	Methylene blue	10	298 K	277.78 mg g^{-1}	–	[212]
			308 K	276.24 mg g^{-1}		
			318 K	272.48 mg g^{-1}		
NH_2-MCM-41	Acid fuchsine	2	25 °C	140.60 mg g^{-1}	–	[213]
			30 °C	134.78 mg g^{-1}		
			40 °C	133.33 mg g^{-1}		
	Acid orange II	3	25 °C	278.38 mg g^{-1}	–	
			30 °C	224.54 mg g^{-1}		
			40 °C	203.56 mg g^{-1}		
PPy/MCM-41	Acid blue 62	2	20 °C	55.55 mg g^{-1}	–	[235]
MSNs	Reactive Black 5	6	–	399.25 mg g^{-1}	–	[236]
MSNs-co-APTES				174.44 mg g^{-1}		
MSNs-post-APTES				436.64 mg g^{-1}		
Si-MCM-41	Basic Red 2	–	303 K	275.5 mg g^{-1}	–	[237]
	Basic Red 5		303 K	288.2 mg g^{-1}		
	Congo Red		313 K	87.4 mg g^{-1}		
	Reactive Red 2		308 K	60.2 mg g^{-1}		
Ni-MCM-41	Methyl blue	6.32	15 °C	121.34 mg g^{-1}	–	[214]
			25 °C	157.48 mg g^{-1}		
			50 °C	181.82 mg g^{-1}		
			80 °C	189.04 mg g^{-1}		
MCM-41 nanoparticle	Acridine Orange	–	–	333.0 mg g^{-1}	–	[238]
	Auramine O			62.5 mg g^{-1}		
Mn_2O_3/MCM-41	Methylene blue	–	–	–	97.5	[239]
	Rhodamine				95.6	
mMCM-41-p(GMA)-TAEA	Direct black 38	5	25 °C	79.9 mg g^{-1}	–	[240]
	Direct Blue 6	6		142.7 mg g^{-1}		
Al-MCM-41 (Si/Al = 25)	Ethylenediaminetetraacetic acid	2	30–32 °C	89.8 mg g^{-1}	89.8	[215]
Al-MCM-41 (Si/Al = 50)				78.6 mg g^{-1}	78.6	
Al-MCM-41 (Si/Al = 75)				71.7 mg g^{-1}	71.7	
Al-MCM-41 (Si/Al = 100)				62.4 mg g^{-1}	62.4	

(*continued on next page*)

Table 2 (*continued*)

Material	Compound	pH	Temperature	Adsorption capacity	Efficiency (%)	Reference
Al-MCM-41 (Si/Al = 25)	Oxalic acid	1	–	58.5 mg g^{-1}	–	[216]
		3		45.6 mg g^{-1}		
		5		36.3 mg g^{-1}		
		7		28.6 mg g^{-1}		
		9		22.7 mg g^{-1}		
		11		19.0 mg g^{-1}		
		13		16.7 mg g^{-1}		
UC-MCM-41	Picric acid	Initial	25 °C	–	82	[217]
Sr-MCM-41	Naphthenic Acid	–	25 °C	2.0 g g^{-1}	–	[241]
MCM-41	Acetaminophen	2	25 °C	121.9 mg g^{-1}	–	[205]
MCM-41-GO	Aspirin			322.6 mg g^{-1}		
MCM-41-G				555.6 mg g^{-1}		
MCM-41				909.1 mg g^{-1}		
MCM-41-GO				714.3 mg g^{-1}		
MCM-41-G				769.2 mg g^{-1}		
Fe-MCM-41	Norfloxacin	7	288 K	134.26 mg g^{-1}	–	[206]
			298 K	102.90 mg g^{-1}		
			308 K	109.34 mg g^{-1}		
Pr-MCM-41	Estrone	7	25 °C	88.38 mg g^{-1}	–	[218]
	17β-estradiol			86.91 mg g^{-1}		
	17α-ethinyl estradiol			119.87 mg g^{-1}		
Fe-MCM-41-A	Tetracycline	5	25 °C	526.3 mg g^{-1}	–	[219]
A-MCM-41	Tetracycline	3	323 K	419 mg g^{-1}	–	[220]
MCM-41 (25 mol%Fe/Si(H))	Acetylsalicylic acid	–	–	7.082 mg g^{-1}	–	[242]
PE-MCM-41	Urease	7.2	–	102 mg g^{-1}	–	[221]
MCM-41				57.6 mg g^{-1}		
MCM-41	Bovine serum albumin	5	–	150 mg g^{-1}	–	[222]
	Lysozyme	7.6		255 mg g^{-1}		
Al^{3+}-MCM-41	DNA	6	–	44.7 mg g^{-1}	90.39	[223]
La^{3+}-MCM-41				42.7 mg g^{-1}	80.88	
Zn^{2+}-MCM-41				36.7 mg g^{-1}	70.40	
MCM-41	DDT	–	–	–	~92	[224]
MCM-41	Diazinon	9	318 K	142 mg g^{-1}	56.4	[243]
MPS-MCM-41				254 mg g^{-1}	87.2	
MCM-41 SiO_2	Paraquat	9.5	25 °C	416 μmol g^{-1}	–	[225]
N-MCM-41	Nitrate	7	25 °C	31.7 mg g^{-1}	–	[228]
NN-MCM-41				38.6 mg g^{-1}		
NNN-MCM-41				38.8 mg g^{-1}		
Amine-MCM-41	Nitrate	–	–	–	56	[149]
MCM-41-CFA-10	Phosphate	–	298 K	64.2 mg g^{-1}	–	[229]
			308 K	51.9 mg g^{-1}		
			318 K	46.2 mg g^{-1}		
MCM-41 silica/rice husk	Phosphate	6	–	21.01 mg g^{-1}	–	[230]
Post-synthesized	Phosphate	–	–	45.162 mg g^{-1}	–	[244]
One-pot synthesized				40.806 mg g^{-1}		
Pure MCM-41				31.123 mg g^{-1}		
MCM-41	Tetraalkyl ammonium hydroxide	9.85	–	1.28 mmol g^{-1}	–	[245]
MCM-41	Nitrobenzene	5.8	25 °C	25.8 μmol g^{-1}	–	[246]
CH_3-MCM-41				375.5 μmol g^{-1}		
MCM-41	Nitrobenzene	5.8	278 K	3.705 μmol g^{-1}	–	[247]
			288 K	2.682 μmol g^{-1}		
			298 K	2.142 μmol g^{-1}		
			308 K	1.841 μmol g^{-1}		

96.9, 88.2, and 88.3 mg CO_2 g^{-1} sample using the MCM-41, PE-MCM-PEI (50), PE-MCM-PEHA (50), and PE-MCM-TEPA (50) mesoporous materials, respectively, in addition, the maximum adsorption amount of 11.39 mmol g^{-1} for MCM-41 and 10.40 mmol g^{-1} for SMCM-41 were obtained by Carvalho et al. [290].

On the other hand, Zhang et al. [291] used the MCM-41, APTMS/MCM-41, PEI/MCM-41, and AAPTS/MCM-41 mesoporous materials for the H_2S removal. The authors found adsorption capacity values of 14.9, 134.4, 40.2, and 46.6 mg^{-1}, respectively, equivalent to the respective removal rate of 21.9, 54.2, 42.1, and 44.8%. Li et al. [292] obtained an adsorption capacity of 0.44 mmol g^{-1} in the remediation of phenanthrene gas by MCM-41, while Li et al. [286] achieved q_m values of 0.094, 0.441, and 0.411 in the removal of gaseous Nap, Phe, and Pyr, respectively, by MCM-41 mesoparticles. Branton et al. [293] performed the removal of CO_2, SO_2, and H_2O vapors by MCM-41 and found adsorption values of 5.1, 3.5, and 1.7 mmol g^{-1} in the temperatures of 195, 273, and 303 K, respectively.

Some works have also been devoted to the removal of gaseous molecules that represent a commercial importance. However, the greatest difficulties are in the processes of storage and transport, in the particular case of hydrogen. Therefore, Pal et al. [294] found removal values of 5.50, 4.00, 10.00, 1.45, 2.10, and 2.45 mmol g^{-1} of H_2 and 0.52, 0.47, 0.58, 0.38, 0.29, and 0.25 mmol g^{-1} of CO_2 by CHMS-1, CHMS-2, CHMS-5, LHMS-1, LHMS-3, and LHMS-5 materials, respectively. Belmabkhout and Sayari [295] obtained adsorptive amount of 145.9, 4.2, 10.4, 434.2, and 14.5 mmol g^{-1} in the CO_2, N_2, CH_4, H_2, and O_2 removal by MCM-41 mesoporous material, respectively. Edler et al. [296] showed adsorption values of 10.0 and 15.8 mmol g^{-1} for N_2 and H_2 by MCM-41 mesoparticles, while Carraro et al. [297] obtained a maximum adsorptive amount for the H_2 removal of 1168, 0.765, and 0.458 wt% for the Ni/MCM-41(1), MCM-41, and Ni/MCM-41(15) materials, respectively. Table 4 presents some MCM-41-based mesoporous materials that were used for the removal of gaseous compounds.

Table 3
Adsorption of various inorganic compound by mesoporous materials.

Material	Compound	pH	Temperature	Maximum adsorption capacity	Efficiency (%)	Reference
α-Fe_2O_3/MCM-41	As(III)	7	298 K	133.3 mg g^{-1}	–	[254]
	As(V)	4		102.1 mg g^{-1}		
MCM-41	Cr(VI)	3.1	–	25.2 mg g^{-1}	–	[255]
	As(V)			18.0 mg g^{-1}		
NH_2/MCM-41/NTAA	Pb^{2+}	5	25 °C	147 mg g^{-1}	98	[257]
	MnO^{4-}	3		156 mg g^{-1}	98	
MP/MCM-41	Pb^{2+}	5	298 K	4.99 mg g^{-1}	99.9	[258]
	Cu^{2+}			39.51 mg g^{-1}	79.0	
	Cd^{2+}			61.00 mg g^{-1}	48.8	
				4.37 mg g^{-1}	87.42	
				35.57 mg g^{-1}	69.15	
				53.38 mg g^{-1}	42.70	
				0.18 mg g^{-1}	3.52	
				1.39 mg g^{-1}	2.78	
				2.15 mg g^{-1}	1.72	
MCM-41	Sr^{2+}	9	–	9.97 mg g^{-1}	> 95	[43]
MCM-41	Hg^{2+}	8	–	163.93 mg g^{-1}	99.52	[259]
CS/MCM-41-PAA	Hg^{2+}	4	298 K	179.43 mg g^{-1}	–	[260]
MCM-41	Pb(II)	5	–	129.87 mg g^{-1}	–	[261]
MCM-41@salen				138.88 mg g^{-1}		
NH_2-MCM-41	Uranium	5	40 °C	625 mg g^{-1}	–	[256]
MCM-41	Uranium	4–8	25 °C	18.08 mg g^{-1}	–	[262]
MCM-41	Cs	2	–	15 mg g^{-1}	–	[263]
MCM-41-SH				30 mg g^{-1}		
NH_2-MCM-41	Cr(VI)	3.5	40 °C	38.55 mg g^{-1}	98.70	[253]
DMDDA-41A	Cu(II)	–	25 °C	1.59 mmol g^{-1}	–	[264]
	Pb(II)			0.41 mmol g^{-1}		
	Cd(II)			0.44 mmol g^{-1}		
	Co(II)			0.73 mmol g^{-1}		
Pristine MCM-41	U(VI)	5	323 K	70.7 mg g^{-1}	–	[265]
MCM-41 (CA)				371.2 mg g^{-1}		
MCM-41 (AMD)				493.6 mg g^{-1}		
Fe_3O_4@MCM-41-NH_2	Pb^{+2}	7	–	46.08 mg g^{-1}	–	[249]
MCM-41/TMSPDETA	Pb(II)	6	20 °C	58.82 mg g^{-1}	–	[266]
	Ni(II)			20.92 mg g^{-1}		
s-MCM-41-NH_2	Cr	2	–	50.8 mg g^{-1}	–	[139]
l-MCM-41-NH_2				37.7 mg g^{-1}		
NN-MCM-41	Cd(II)	–	25 °C	64.93 mg g^{-1}	–	[267]
	Co(II)			103.09 mg g^{-1}		
	Cu(II)			172.41 mg g^{-1}		
	Pb(II)			169.49 mg g^{-1}		
Pyridine-MCM-41	Ni(II)	7	–	83.0 mg g^{-1}	–	[268]
(20)TiO_2-MCM-41	Cr(VI)	~5.5	323 K	–	91	[269]
Magnetic MCM-41	Cr	2	298 K	99 mg g^{-1}	–	[270]
		5		83 mg g^{-1}		
NH_2-MCM-41	Cr(VI)	2	25 °C	60.91 mg g^{-1}	–	[271]
			35 °C	80.06 mg g^{-1}		
			45 °C	82.05 mg g^{-1}		
SDS-MCM-41	Cd^{2+}	7	–	8.56 mg g^{-1}	–	[272]
	Cu^{2+}			9.51 mg g^{-1}		
	Zn^{2+}			5.78 mg g^{-1}		
CS-MCM-41-A	Pb(II)	6	–	–	99.83	[140]
MCM-41-NH-L	Hg(II)	3	298 K	0.70 mmol g^{-1}	–	[273]
MTTZ-MCM-41	Zn^{2+}	8	–	1.59 mmol g^{-1}	–	[274]
MBT-MCM-41-Het	Hg(II)	6	25 °C	0.13 mmol g^{-1}	–	[275]
MBT-MCM-41-Hom				0.21 mmol g^{-1}		
DT-MCM-41	Hg^{2+}	6	25 °C	538.9 mg g^{-1}	> 99	[276]
APTS-MCM-41/PMMA	Cd(II)	5	25 °C	24.75 mg g^{-1}	–	[277]
APTS-MCM-41/PS				10.42 mg g^{-1}		
PEI/MCM-41	Cd(II)	6.0	30 °C	156.0 mg g^{-1}	–	[278]
	Ni(II)			139.7 mg g^{-1}		
M-MCM-41/PVOH NC	Cd(II)	6.0	–	46.73 mg g^{-1}	–	[127]
$ZnCl_2$-MCM-41	Hg(II)	10	20 °C	204.1 mg g^{-1}	–	[42]
c-MCM-41(40)	Cu^{2+}	5–7	–	36.3 mg g^{-1}	–	[279]
	Pb^{2+}			58.5 mg g^{-1}		
	Cd^{2+}			32.3 mg g^{-1}		
MCM-41-NH_2	Cr(VI)	2	45 °C	97.8 mg g^{-1}	–	[280]
	Zn(II)	7		73.8 mg g^{-1}		
MnO_2/MCM-41	Cr(VI)	2	328 K	4.111 mg g^{-1}	–	[281]
	As(III)	4		2.968 mg g^{-1}		
NH_2-MCM-41	As(III)	5.62	25 °C	5.8360 mg g^{-1}	–	[282]
			30 °C	5.8697 mg g^{-1}		
			40 °C	5.8916 mg g^{-1}		

(*continued on next page*)

Table 3 (*continued*)

Material	Compound	pH	Temperature	Maximum adsorption capacity	Efficiency (%)	Reference
MCM-41	Cu^{2+}	–	30 °C	0.13 mmol g^{-1}	–	[283]
MCM-41N1				0.44 mmol g^{-1}		
MCM-41N2				0.76 mmol g^{-1}		
MCM-41N3				0.93 mmol g^{-1}		

5. Conclusions

In this work, the most recent research progress on the adsorption of organic, inorganic, and gas compounds by MCM-41-based mesoporous material has been thoroughly reviewed, as well as the main variables in the preparation of mesoporous materials and the methods of

Table 4
Adsorption of gas compound by mesoporous materials.

Material	Compound	Temperature	Maximum adsorption capacity	Efficiency (%)	Reference
5A-MCM-41 composite	CO_2	298 K	4.08 mmol g^{-1}	–	[287]
MCM-41-TEPA60%	CO_2	70 °C	2.45 mmol g^{-1}	–	[288]
MCM-41-APTS30%-TEPA40%			3.50 mmol g^{-1}		
MCM-41	CO_2	303 K	14.2 mmol g^{-1}	–	[289]
MCM-41/Cu(BDC)	CH_4		14.15 mmol g^{-1}		
	CO_2		40.82 mmol g^{-1}		
	CH_4		36 mmol g^{-1}		
MCM-41	CO_2	–	16.1 mg g^{-1}	–	[160]
PE-MCM-PEI (50)			96.9 mg g^{-1}		
PE-MCM-PEHA (50)			88.2 mg g^{-1}		
PE-MCM-TEPA (50)			88.3 mg g^{-1}		
MCM-41	CO_2	–	11.39 mmol g^{-1}	–	[290]
SMCM-41			10.40 mmol g^{-1}		
MCM-41	H_2S	–	14.9 mg g^{-1}	21.9	[291]
APTMS/MCM-41			134.4 mg g^{-1}	54.2	
PEI/MCM-41			40.2 mg g^{-1}	42.1	
AAPTS/MCM-41			46.6 mg g^{-1}	44.8	
MCM-41	Phe	125 °C	0.44 mmol g^{-1}	–	[292]
MCM-41	Nap	–	0.094 mmol g^{-1}	–	[286]
	Phe		0.441 mmol g^{-1}		
	Pyr		0.411 mmol g^{-1}		
MCM-41	CO_2	195 K	5.1 mmol g^{-1}	–	[293]
	SO_2	273 K	3.5 mmol g^{-1}		
	H_2O	303 K	1.7 mmol g^{-1}		
CHMS-1	H_2	–	5.50 mmol g^{-1}	–	[294]
CHMS-2	CO_2		4.00 mmol g^{-1}		
CHMS-5			10.00 mmol g^{-1}		
LHMS-1			1.45 mmol g^{-1}		
LHMS-3			2.10 mmol g^{-1}		
LHMS-5			2.45 mmol g^{-1}		
CHMS-1			0.52 mmol g^{-1}		
CHMS-2			0.47 mmol g^{-1}		
CHMS-5			0.58 mmol g^{-1}		
LHMS-1			0.38 mmol g^{-1}		
LHMS-3			0.29 mmol g^{-1}		
LHMS-5			0.25 mmol g^{-1}		
MCM-41	CO_2	298 K	145.9 mmol g^{-1}		[295]
	N_2		4.2 mmol g^{-1}		
	CH_4		10.4 mmol g^{-1}		
	H_2		434.2 mmol g^{-1}		
	O_2		14.5 mmol g^{-1}		
MCM-41	N_2	–	10.0 mmol g^{-1}	–	[296]
	H_2		15.8 mmol g^{-1}		
Ni/MCM-41(1)	H_2	77 K	1168 wt%		[297]
MCM-41			0.765 wt%		
Ni/MCM-41(15)			0.458 wt%		
TRI-PE-MCM-41	CO_2	298 K	1.75 mmol g^{-1}	–	[298]
DIPA-MCM-41	CO_2	–	0.017 mol g^{-1}	–	[299]
RH-MCM-41 (TMCS-M)	BTEX	–	123.2 μmol g^{-1}	–	[284]
TEPA-Si-MCM-41 (50 wt%)	CO_2	75 °C	70.41 mg g^{-1}	–	[133]
MCM-41 (C18F)	Benzene *n*-hexene	298 K	0.86 cm^3 g^{-1}	–	[300]
	Neopentane	298 K	0.86 cm^3 g^{-1}		
	Methanol	273 K	0.86 cm^3 g^{-1}		
	Nitrogen	298 K	0.88 cm^3 g^{-1}		
		77 K	0.90 cm^3 g^{-1}		
50% PEI – MCM-41	CO_2	25 °C	3.53 mmol g^{-1}	–	[44]
50% APTS – MCM-41			2.41 mmol g^{-1}		
MCM-41	Acetone	523 K	~1.5 mmol g^{-1}	–	[301]
MCM-41	Nap	125 °C	0.094 mol kg^{-1}	–	[302]

functionalization most used to prepare MCM-41-based functionalized mesoporous materials and finally the factors that affect the adsorption process. In view of this, it is possible to state that adsorption technology has attracted a lot of attention in the removal of environmental pollutants, mainly due to the fact that it is a technique that requires the use of few steps and equipment, easy operation, low cost, does not generate residues or by-products, and high energy efficiency, allowing the use of this technique in environmental remediation process.

This work demonstrates that satisfactory progress has been achieved in the adsorption technology of the most different pollutants and in the most different pollution sources from the use of mesoporous materials, especially MCM-41-based mesoporous arrays, considering the main textural and structural features of MCM-41, which allow its wide application in the adsorption technology.

Conflicts of interest

The authors declare that they have no conflict of interest.

Acknowledgments

The authors thank Fundação de Amparo à Pesquisa do Estado de São Paulo (FAPESP, Grants 2014/05679-4, 2017/06775-5, and 2018/18894-1), Coordenação de Aperfeiçoamento de Pessoal de Nível Superior (CAPES, Grant 309342/2010-4), Conselho Nacional de Desenvolvimento Científico e Tecnológico (CNPq, Grant 303418/2016-8), and Centro de Desenvolvimento de Materiais Funcionais (CDMF, Grant 2013/07296-2) for the financial support.

References

[1] T. Blasco, A. Corma, M.T. Navarro, J. Pérez Pariente, Synthesis, characterization, and catalytic activity of TI-MCM-41 structures, J. Catal. 156 (1995) 65–74, https://doi.org/10.1006/jcat.1995.1232.
[2] V.R. Elías, M.I. Oliva, E.G. Vaschetto, S.E. Urreta, G.A. Eimer, S.P. Silvetti, Magnetic properties of iron loaded MCM-48 molecular sieves, J. Magn. Magn. Mater. 322 (2010) 3438–3442, https://doi.org/10.1016/j.jmmm.2010.06.041.
[3] C. Liu, S. Wang, Z. Rong, X. Wang, G. Gu, W. Sun, Synthesis of structurally stable MCM-48 using mixed surfactants as co-template and adsorption of vitamin B12 on the mesoporous MCM-48, J. Non-Cryst. Solids 356 (2010) 1246–1251, https://doi.org/10.1016/j.jnoncrysol.2010.04.028.
[4] F.N. Murrieta-Rico, P. Mercorelli, O.Y. Sergiyenko, V. Petranovskii, D. Hernandez-Balbuena, V. Tyrsa, Mathematical Modelling of molecular adsorption in zeolite coated frequency domain sensors, IFAC-PapersOnLine. 28 (2015) 41–46, https://doi.org/10.1016/j.ifacol.2015.05.060.
[5] Z. Karimi, M. Shamsipur, M.A. Tabrizi, S. Rostamnia, A highly sensitive electrochemical sensor for the determination of methanol based on PdNPs@SBA-15-PrEn modified electrode, Anal. Biochem. 548 (2018) 32–37, https://doi.org/10.1016/j.ab.2018.01.033.
[6] A.-M. Brezoiu, M. Deaconu, I. Nicu, E. Vasile, R.-A. Mitran, C. Matei, D. Berger, Heteroatom modified MCM-41-silica carriers for Lomefloxacin delivery systems, Microporous Mesoporous Mater. 275 (2019) 214–222, https://doi.org/10.1016/j.micromeso.2018.08.031.
[7] C.T. Kresge, M.E. Leonowicz, W.J. Roth, J.C. Vartuli, J.S. Beck, Ordered mesoporous molecular sieves synthesized by a liquid-crystal template mechanism, Nature 359 (1992) 710–712.
[8] J.S. Beck, J.C. Vartuli, W.J. Roth, M.E. Leonowicz, C.T. Kresge, K.D. Schmitt, C.T.-W. Chu, D.H. Olson, E.W. Sheppard, S.B. McCullen, J.B. Higgins, J.L. Schlenkert, A new family of mesoporous molecular sieves prepared with liquid crystal templates, J. Am. Chem. Soc. (1992) 10834–10843, https://doi.org/10.1021/ja00053a020.
[9] C.T. Kresge, J.C. Vartuli, W.J. Roth, M.E. Leonowicz, The discovery of ExxonMobil's M41S family of mesoporous molecular sieves, Stud. Surf. Sci. Catal. 148 (2004) 53–72, https://doi.org/10.1016/S0167-2991(04)80193-9.
[10] V. Zeleňák, M. Badaničová, D. Halamová, J. Čejka, A. Zukal, N. Murafa, G. Goerigk, Amine-modified ordered mesoporous silica: effect of pore size on carbon dioxide capture, Chem. Eng. J. 144 (2008) 336–342, https://doi.org/10.1016/j.cej.2008.07.025.
[11] J.C. Vartuli, K.D. Schmitt, C.T. Kresge, W.J. Roth, M.E. Leonowicz, S.B. McCullen, S.D. Hellring, J.S. Beck, J.L. Schlenker, D.H. Olson, E.W. Sheppard, Development of a formation mechanism for M41S materials, Stud. Surf. Sci. Catal. 84 (1994) 53–60, https://doi.org/10.1016/S0167-2991(08)64096-3.
[12] M. Dubois, T. Gulik-Krzywicki, B. Cabane, Growth of silica polymers in a lamellar mesophase, Langmuir 9 (1993) 673–680, https://doi.org/10.1021/la00027a011.
[13] A. Sayari, S. Hamoudi, Periodic mesoporous silica-based organic-inorganic nanocomposite materials, Chem. Mater. 13 (2001) 3151–3168.
[14] M. Pérez-Mendoza, J. Gonzalez, P.A. Wright, N.A. Seaton, Structure of the mesoporous silica SBA-2, determined by a percolation analysis of adsorption, Langmuir 20 (2004) 9856–9860, https://doi.org/10.1021/la0493159.
[15] D. Zhao, J. Sun, Q. Li, G.D. Stucky, Morphological control of highly ordered mesoporous silica SBA-15, Chem. Mater. 12 (2000) 275–279, https://doi.org/10.1021/cm9911363.
[16] J. Puputti, H. Jin, J. Rosenholm, H. Jiang, M. Lindén, The use of an impure inorganic precursor for the synthesis of highly siliceous mesoporous materials under acidic conditions, Microporous Mesoporous Mater. 126 (2009) 272–275, https://doi.org/10.1016/j.micromeso.2009.06.017.
[17] E.M. Björk, Synthesizing and characterizing mesoporous silica SBA-15: a hands-on laboratory experiment for undergraduates using various instrumental techniques, J. Chem. Educ. 94 (2017) 91–94, https://doi.org/10.1021/acs.jchemed.5b01033.
[18] V. Malgras, H. Ataee-Esfahani, H. Wang, B. Jiang, C. Li, K.C.W. Wu, J.H. Kim, Y. Yamauchi, Nanoarchitectures for mesoporous metals, Adv. Mater. 28 (2016) 993–1010, https://doi.org/10.1002/adma.201502593.
[19] S. Salimian, A. Zadhoush, A. Mohammadi, A review on new mesostructured composite materials: Part I. synthesis of polymer-mesoporous silica nanocomposite, J. Reinf. Plast. Compos. 37 (2018) 441–459, https://doi.org/10.1177/0731684417752081.
[20] A.A.C. Braga, I. Català, C. Espanha, N.H. Morgon, CAI as a teaching tool for occupational therapy, dissertation 30 (2007) 178–188.
[21] R.M. Barrer, D.W. Brook, Molecular diffusion in chabazite, mordenite and levynite, Trans. Faraday Soc. 49 (1953) 1049–1059, https://doi.org/10.1039/tf9534901049.
[22] J.W. McBain, The sorption of gases and vapours by solids, J. Phys. Chem. 37 (1932) 149–150, https://doi.org/10.1021/j150343a021.
[23] U. Ciesla, F. Schüth, Ordered mesoporous materials, Microporous Mesoporous Mater. 27 (1999) 131–149, https://doi.org/10.1016/S1387-1811(98)00249-2.
[24] M. Estermann, L.B. McCusker, C. Baerlocher, A. Merrouche, H. Kessler, A synthetic gallophosphate molecular sieve with a 20-tetrahedral-atom pore opening, Nature 352 (1991) 320–323, https://doi.org/10.1038/352320a0.
[25] M.E. Davis, R.F. Lobo, Zeolite and molecular sieve synthesis, Chem. Mater. 4 (1992) 756–768, https://doi.org/10.1021/cm00022a005.
[26] G.A. Ozin, Nanochemistry: synthesis in diminishing dimensions, Adv. Mater. 4 (1992) 612–649, https://doi.org/10.1002/adma.19920041003.
[27] H.J. Kim, K.S. Jang, P. Galebach, C. Gilbert, G. Tompsett, W.C. Conner, C.W. Jones, S. Nair, Seeded growth, silylation, and organic/water separation properties of MCM-48 membranes, J. Membr. Sci. 427 (2013) 293–302, https://doi.org/10.1016/j.memsci.2012.10.012.
[28] S.T. Wilson, B.M. Lok, C.A. Messina, T.R. Cannan, E.M. Flanigen, Aluminophosphate molecular sieves: a new class of microporous crystalline inorganic solids, J. Am. Chem. Soc. 104 (1982) 1146–1147, https://doi.org/10.1021/ja00368a062.
[29] M.E. Davis, C. Saldarriaga, C. Montes, J. Garces, C. Crowdert, A molecular sieve with eighteen-membered rings, Nature 331 (1988) 698–699, https://doi.org/10.1038/331698a0.
[30] R.H. Jones, J.M. Thomas, J. Chen, R. Xu, Q. Huo, S. Li, Z. Ma, A.M. Chippindale, Structure of an unusual aluminium phosphate ([Al5P6O24H]2—2[N(C2H5)3H] +· 2H2o) jdf-20 with large elliptical apertures, J. Solid State Chem. 102 (1993) 204–208, https://doi.org/10.1006/jssc.1993.1023.
[31] T. Yanagisawa, T. Shimizu, K. Kuroda, C. Kato, The preparation of alkyltrimethylammonium-kanemite complexes and their conversion to microporous materials, Bull. Chem. Soc. Jpn. 63 (1990) 988–992, https://doi.org/10.1246/bcsj.63.988.
[32] M.J.B. Souza, A.M. Garrido Pedrosa, J.A. Cecilia, A.M. Gil-Mora, E. Rodríguez-Castellón, Hydrodesulfurization of dibenzothiophene over PtMo/MCM-48 catalysts, Catal. Commun. 69 (2015) 217–222, https://doi.org/10.1016/j.catcom.2015.07.004.
[33] L. Pajchel, W. Kolodziejski, Synthesis and characterization of MCM-48/hydroxyapatite composites for drug delivery: ibuprofen incorporation, location and release studies, Mater. Sci. Eng. C 91 (2018) 734–742, https://doi.org/10.1016/j.msec.2018.06.028.
[34] N. Cakiryilmaz, H. Arbag, N. Oktar, G. Dogu, T. Dogu, Catalytic performances of Ni and Cu impregnated MCM-41 and Zr-MCM-41 for hydrogen production through steam reforming of acetic acid, Catal. Today 323 (2018) 191–199, https://doi.org/10.1016/j.cattod.2018.06.004.
[35] A.K. Basumatary, A.K. Ghoshal, G. Pugazhenthi, Performance assessment of MCM-48 ceramic composite membrane by separation of AlCl3from aqueous solution, Ecotoxicol. Environ. Saf. 134 (2016) 398–402, https://doi.org/10.1016/j.ecoenv.2015.10.010.
[36] L.F.S. Santos, R.A. de Jesus, J.A.S. Costa, L.G.T. Gouveia, M.E. de Mesquita, S. Navickiene, Evaluation of MCM-41 and MCM-48 mesoporous materials as sorbents in matrix solid phase dispersion method for the determination of pesticides in soursop fruit (Annona muricata), Inorg. Chem. Commun. 101 (2019) 45–51, https://doi.org/10.1016/j.inoche.2019.01.013.
[37] D.O. Santos, M.L.N. Santos, J.A.S. Costa, R.A. de Jesus, S. Navickiene, E.M. Sussuchi, M.E. de Mesquita, Investigating the potential of functionalized MCM-41 on adsorption of Remazol Red dye, Environ. Sci. Pollut. Res. 20 (2013) 5028–5035, https://doi.org/10.1007/s11356-012-1346-6.
[38] J.A.S. Costa, R.A. de Jesus, C.M.P. da Silva, L.P.C. Romão, Efficient adsorption of a mixture of polycyclic aromatic hydrocarbons (PAHs) by Si–MCM–41 mesoporous molecular sieve, Powder Technol. 308 (2017) 434–441, https://doi.org/10.1016/j.powtec.2016.12.035.
[39] R. Schmidt, M. Stöcker, E. Hansen, D. Akporiaye, O.H. Ellestad, MCM-41: a model system for adsorption studies on mesoporous materials, Microporous Mater. 3 (1995) 443–448, https://doi.org/10.1016/0927-6513(94)00055-Z.

[40] K.K. Kang, C.S. Byun, W.S. Ahn, Titanium iso-propoxide grafting on M41S type hosts: catalytic and adsorption study, Stud. Surf. Sci. Catal. 129 (2000) 335–340.

[41] M. Algarra, M.V. Jiménez, E. Rodríguez-Castellón, A. Jiménez-López, J. Jiménez-Jiménez, Heavy metals removal from electroplating wastewater by aminopropyl-Si MCM-41, Chemosphere 59 (2005) 779–786, https://doi.org/10.1016/j.chemosphere.2004.11.023.

[42] F. Raji, M. Pakizeh, Study of Hg(II) species removal from aqueous solution using hybrid ZnCl2-MCM-41 adsorbent, Appl. Surf. Sci. 282 (2013) 415–424, https://doi.org/10.1016/j.apsusc.2013.05.145.

[43] M.S. Yilmaz, Ö.D. Özdemir, S. Pişkin, Synthesis and characterization of MCM-41 with different methods and adsorption of Sr2 + on MCM-41, Res. Chem. Intermed. 41 (2015) 199–211, https://doi.org/10.1007/s11164-013-1182-4.

[44] N. Rao, M. Wang, Z. Shang, Y. Hou, G. Fan, J. Li, CO2 adsorption by amine-functionalized MCM-41: a comparison between impregnation and grafting modification methods, Energy Fuel. 32 (2018) 670–677, https://doi.org/10.1021/acs.energyfuels.7b02906.

[45] Z. Cheng, B. Yang, Q. Chen, W. Ji, Z. Shen, Characteristics and difference of oxidation and coagulation mechanisms for the removal of organic compounds by quantum parameter analysis, Chem. Eng. J. 332 (2018) 351–360, https://doi.org/10.1016/J.CEJ.2017.09.065.

[46] R. Qi, X. Lin, J. Dai, H. Zhao, S. Liu, T. Fei, T. Zhang, Humidity sensors based on MCM-41/polypyrrole hybrid fi lm via in-situ polymerization, Sens. Actuators B Chem. 277 (2018) 584–590.

[47] B.M. Abu-Zied, M.M. Alam, A.M. Asiri, W. Schwieger, M.M. Rahman, Fabrication of 1,2-dichlorobenzene sensor based on mesoporous MCM-41 material, Colloids Surfaces A Physicochem. Eng. Asp. 562 (2019) 161–169, https://doi.org/10.1016/j.colsurfa.2018.11.024.

[48] R.A. Jesus, A.S. Rabelo, R.T. Figueiredo, L.C. Cides Da Silva, I.C. Codentino, M.C.A. Fantini, G.L.B. Araújo, A.A.S. Araújo, M.E. Mesquita, Synthesis and application of the MCM-41 and SBA-15 as matrices for in vitro efavirenz release study, J. Drug Deliv. Sci. Technol. 31 (2016) 153–159, https://doi.org/10.1016/j.jddst.2015.11.008.

[49] P.V. Shah, S.J. Rajput, A comparative in vitro release study of raloxifene encapsulated ordered MCM-41 and MCM-48 nanoparticles: a dissolution kinetics study in simulated and biorelevant media, J. Drug Deliv. Sci. Technol. 41 (2017) 31–44, https://doi.org/10.1016/j.jddst.2017.06.015.

[50] A. Sayari, Periodic mesoporous materials: synthesis, characterization and potential applications, Stud. Surf. Sci. Catal. 102 (1996) 1–46.

[51] J.A.S. Costa, P. Vedovello, C.M. Paranhos, Use of Ionic Liquid as Template for Hydrothermal Synthesis of the MCM-41 Mesoporous Material, Silicon, (2019), https://doi.org/10.1007/s12633-019-00121-9.

[52] S.E. Park, D.S. Kim, J.S. Chang, W.Y. Kim, Synthesis of MCM-41 using microwave heating with ethylene glycol, Catal. Today 44 (1998) 301–308, https://doi.org/10.1016/S0920-5861(98)00203-X.

[53] H. Chen, Y.P. Peng, K.F. Chen, C.H. Lai, Y.C. Lin, Rapid synthesis of Ti-MCM-41 by microwave-assisted hydrothermal method towards photocatalytic degradation of oxytetracycline, J. Environ. Sci. (China) 44 (2016) 76–87, https://doi.org/10.1016/j.jes.2015.08.027.

[54] A.N. Ergün, Z.Ö. Kocabaş, M. Baysal, A. Yürüm, Y. Yürüm, Synthesis OF mesoporous MCM-41 materials with low-power microwave heating, Chem. Eng. Commun. 200 (2013) 1057–1070, https://doi.org/10.1080/00986445.2012.737386.

[55] E. Dündar-Tekkaya, Y. Yürüm, Effect of loading bimetallic mixture of Ni and Pd on hydrogen storage capacity of MCM-41, Int. J. Hydrogen Energy 40 (2015) 7636–7643, https://doi.org/10.1016/j.ijhydene.2015.02.108.

[56] G. Gheno, N.R.D.S. Basso, P.R. Livotto, M.R. Ribeiro, J.P. Lourenço, A.E. Ferreira, G.B. Galland, A new post-metallocene-Ti catalyst with maltolate bidentade ligand: an investigation in heterogeneous polymerization reactions in different mesoporous supports, J. Braz. Chem. Soc. 27 (2016) 2082–2092, https://doi.org/10.5935/0103-5053.20160099.

[57] G.G. Lara, G.F. Andrade, M.F. Cipreste, W.M. da Silva, P.L. Gastelois, D.A. Gomes, M.C. de Miranda, W.A. de Almeida Macedo, M.J. Neves, E.M.B. de Sousa, Protection of normal cells from irradiation bystander effects by silica-flufenamic acid nanoparticles, J. Mater. Sci. Mater. Med. 29 (2018), https://doi.org/10.1007/s10856-018-6134-5.

[58] P. Kumar, N. Mal, Y. Oumi, K. Yamana, T. Sano, Mesoporous materials prepared using coal fly ash as the silicon and aluminium source, J. Mater. Chem. 11 (2001) 3285–3290, https://doi.org/10.1039/b104810b.

[59] R. Tayebee, M.M. Amini, M. Akbari, A. Aliakbari, A novel inorganic-organic nanohybrid material H4SiW12O40/pyridino-MCM-41 as efficient catalyst for the preparation of 1-amidoalkyl-2-naphthols under solvent-free conditions, Dalton Trans. 44 (2015) 9596–9609, https://doi.org/10.1039/c5dt00368g.

[60] S. Brunauer, P.H. Emmett, E. Teller, Adsorption of gases in multimolecular layers, J. Am. Chem. Soc. 60 (1938) 309–319 doi:citeulike-article-id:4074706\ 10.1021/ja01269a023.

[61] E.P. Barrett, L.G. Joyner, P.P. Halenda, The determination of pore volume and area distributions in porous substances. I. Computations from nitrogen isotherms, J. Am. Chem. Soc. 73 (1951) 373–380, https://doi.org/10.1021/ja01145a126.

[62] M. Thommes, K. Kaneko, A.V. Neimark, J.P. Olivier, F. Rodriguez-Reinoso, J. Rouquerol, K.S.W. Sing, Physisorption of gases, with special reference to the evaluation of surface area and pore size distribution (IUPAC Technical Report), Pure Appl. Chem. 87 (2015) 1051–1069, https://doi.org/10.1515/pac-2014-1117.

[63] S. Sohrabnezhad, A. Jafarzadeh, A. Pourahmad, Synthesis and characterization of MCM-41 ropes, Mater. Lett. 212 (2018) 16–19, https://doi.org/10.1016/j.matlet.2017.10.059.

[64] C.Y. Chen, S.L. Burkett, H.X. Li, M.E. Davis, Studies on mesoporous materials II. Synthesis mechanism of MCM-41, Microporous Mater. 2 (1993) 27–34, https://doi.org/10.1016/0927-6513(93)80059-4.

[65] Y. Feng, N. Panwar, D.J.H. Tng, S.C. Tjin, K. Wang, K.T. Yong, The application of mesoporous silica nanoparticle family in cancer theranostics, Coord. Chem. Rev. 319 (2016) 86–109, https://doi.org/10.1016/j.ccr.2016.04.019.

[66] S.P. Naik, S.P. Elangovan, T. Okubo, I. Sokolov, Morphology control of mesoporous silica particles, J. Phys. Chem. C 111 (2007) 11168–11173, https://doi.org/10.1021/jp072184a.

[67] H.P. Lin, S.B. Liu, C.Y. Mou, C.Y. Tang, Hierarchical organization of mesoporous MCM-41 ropes, Chem. Commun. (1999) 583–584, https://doi.org/10.1039/a809767d.

[68] Q. Cai, W.Y. Lin, F.S. Xiao, W.Q. Pang, X.H. Chen, B.S. Zou, The preparation of highly ordered MCM-41 with extremely low surfactant concentration, Microporous Mesoporous Mater. 32 (1999) 1–15, https://doi.org/10.1016/S1387-1811(99)00082-7.

[69] Q. Huo, D.I. Margolese, U. Ciesla, D.G. Demuth, P. Feng, T.E. Gier, P. Sieger, A. Firouzi, B.F. Chmelka, Organization of organic molecules with inorganic molecular species into nanocomposite biphase Arrays, Chem. Mater. 6 (1994) 1176–1191, https://doi.org/10.1021/cm00044a016.

[70] F.H.P. Silva, H.O. Pastore, The syntheses of mesoporous molecular sieves in fluoride medium, Chem. Commun. (1996) 833, https://doi.org/10.1039/cc9960000833.

[71] S. Zhai, J. Zheng, J. Li, D. Wu, Y. Sun, F. Deng, Treatment of calcined MSU-S with NaAlO2 solution in the presence of CTAB: change of acidic and catalytic properties, Microporous Mesoporous Mater. 83 (2005) 10–18 https://doi.org/10.1016/j.micromeso.2005.03.016.

[72] J.T. Tompkins, R. Mokaya, Steam stable mesoporous silica MCM-41 stabilized by trace amounts of Al, ACS Appl. Mater. Interfaces 6 (2014) 1902–1908, https://doi.org/10.1021/am404911x.

[73] C. Galacho, M.M.L. Ribeiro Carrott, P.J.M. Carrott, Evaluation of the thermal and mechanical stability of Si-MCM-41 and Ti-MCM-41 synthesised at room temperature, Microporous Mesoporous Mater. 108 (2008) 283–293, https://doi.org/10.1016/j.micromeso.2007.04.010.

[74] E.A. Karakhanov, A.P. Glotov, A.G. Nikiforova, A.V. Vutolkina, A.O. Ivanov, S.V. Kardashev, A.L. Maksimov, S.V. Lysenko, Catalytic cracking additives based on mesoporous MCM-41 for sulfur removal, Fuel Process. Technol. 153 (2016) 50–57, https://doi.org/10.1016/j.fuproc.2016.07.023.

[75] X.S. Zhao, G.Q. Lu, Modification of MCM-41 by surface silylation with trimethylchlorosilane and adsorption study, J. Phys. Chem. B 102 (1998) 1556–1561, https://doi.org/10.1021/jp972788m.

[76] D. Zhao, J. Feng, Q. Huo, N. Melosh, G.H. Fredrickson, B.F. Chmelka, G.D. Stucky, Triblock copolymer syntheses of mesoporous silica with periodic 50 to 300 angstrom pores, 80-, Science 279 (1998), https://doi.org/10.1126/science.279.5350.548 548 LP – 552.

[77] L. Shi-quan, E.F. Vansant, J. Min-hua, Different routes to the pore engineering of spherical MCM-41, J. Wuhan Univ. Technol. Sci. Ed. 18 (2003) 1–5, https://doi.org/10.1007/BF02838788.

[78] R. Franchi, P.J.E. Harlick, A. Sayari, A high capacity, water tolerant adsorbent for CO2: diethanolamine supported on pore-expanded MCM-41, in: A. Sayari, M.B.T.-S. in S.S, C. Jaroniec (Eds.), Nanoporous Mater. IV, Elsevier, 2005, pp. 879–886, , https://doi.org/10.1016/S0167-2991(05)80300-3.

[79] S.S. Park, J.H. Park, J.H. Park, S.S. Hong, H.C. Park, G.D. Lee, The preparation of fibrous MCM-41 using microwave heating, Key Eng. Mater. 336–338 (2007) 1316–1319 https://doi.org/10.4028/www.scientific.net/KEM.336-338.1316.

[80] L. Li, S. Yu, F. Liu, J. Yang, S. Zhaug, Reactions of turpentine using Zr-MCM-41 family mesoporous molecular sieves, Catal. Lett. 100 (2005) 227–233, https://doi.org/10.1007/s10562-005-3460-2.

[81] A. Corma, From microporous to mesoporous molecular sieve materials and their use in catalysis, Chem. Rev. 97 (1997) 2373–2419, https://doi.org/10.1021/CR960406N.

[82] H.I. Meléndez-Ortiz, Y.A. Perera-Mercado, G. Castruita, J.A. Mercado-Silva, L.A. García-Cerda, Y. Olivares-Maldonado, Preparation of spherical MCM-41 molecular sieve at room temperature: influence of the synthesis conditions in the structural properties, Ceram. Int. 38 (2012) 6353–6358, https://doi.org/10.1016/j.ceramint.2012.05.007.

[83] E. Kaya, N. Oktar, G. Karakas, K. Murtezaoglu, Synthesis and characterization of Ba/MCM-41, Turk. J. Chem. 34 (2010) 935–943, https://doi.org/10.3906/kim-1003-2.

[84] V. Meynen, P. Cool, E.F. Vansant, Verified syntheses of mesoporous materials, Microporous Mesoporous Mater. 125 (2009) 170–223, https://doi.org/10.1016/j.micromeso.2009.03.046.

[85] B.P. Feuston, J.B. Higgins, Model structures for MCM-41 materials: a molecular dynamics simulation, J. Phys. Chem. 98 (1994) 4459–4462, https://doi.org/10.1021/j100067a037.

[86] J.A.S. Costa, A.C.F.S. Garcia, D.O. Santos, V.H. V Sarmento, A.L.M. Porto, M.E. De Mesquita, L.P.C. Romão, A new functionalized MCM-41 mesoporous material for use in environmental applications, J. Braz. Chem. Soc. 25 (2014) 197–207, https://doi.org/10.5935/0103-5053.20130284.

[87] J.A.S. Costa, A.C.F.S. Garcia, D.O. Santos, V.H. V Sarmento, M.E. de Mesquita, L.P.C. Romão, Applications of inorganic-organic mesoporous materials constructed by self-assembly processes for removal of benzo[k]fluoranthene and benzo[b]fluoranthene, J. Sol. Gel Sci. Technol. 75 (2015) 495–507, https://doi.org/10.1007/s10971-015-3720-6.

[88] F. Kleitz, W. Schmidt, F. Schüth, Calcination behavior of different surfactant-templated mesostructured silica materials, Microporous Mesoporous Mater. 65

(2003) 1–29 https://doi.org/10.1016/S1387-1811(03)00506-7.
[89] M.T.J. Keene, R. Denoyel, P.L. Llewellyn, Ozone treatment for the removal of surfactant to form MCM-41 type materials, Chem. Commun. (1998) 2203–2204, https://doi.org/10.1039/A806118A.
[90] B. Tian, X. Liu, C. Yu, F. Gao, Q. Luo, S. Xie, B. Tu, D. Zhao, Microwave assisted template removal of siliceous porous materials, Chem. Commun. (2002) 1186–1187, https://doi.org/10.1039/b202180c.
[91] T.F. Parangi, R.M. Patel, U.V. Chudasama, Synthesis and characterization of mesoporous Si-MCM-41 materials and their application as solid acid catalysts in some esterification reactions, Bull. Mater. Sci. 37 (2014) 609–615, https://doi.org/10.1007/s12034-014-0709-7.
[92] M.T.J. Keene, R.D.M. Gougeon, R. Denoyel, R.K. Harris, J. Rouquerol, P.L. Llewellyn, Calcination of the MCM-41 mesophase: mechanism of surfactant thermal degradation and evolution of the porosity, J. Mater. Chem. 9 (1999) 2843–2849, https://doi.org/10.1039/A904937A.
[93] M. Kruk, M. Jaroniec, Y. Sakamoto, O. Terasaki, R. Ryoo, C.H. Ko, Determination of pore size and pore wall structure of MCM-41 by using nitrogen adsorption, transmission electron microscopy, and X-ray diffraction, J. Phys. Chem. B 104 (2000) 292–301, https://doi.org/10.1021/jp992718a.
[94] H.T. Gomes, P. Selvam, S.E. Dapurkar, J.L. Figueiredo, J.L. Faria, Transition metal (Cu, Cr, and V) modified MCM-41 for the catalytic wet air oxidation of aniline, Microporous Mesoporous Mater. 86 (2005) 287–294 https://doi.org/10.1016/j.micromeso.2005.07.022.
[95] L.Y. Chen, Z. Ping, G.K. Chuah, S. Jaenicke, G. Simon, A comparison of post-synthesis alumination and sol-gel synthesis of MCM-41 with high framework aluminum content, Microporous Mesoporous Mater. 27 (1999) 231–242 https://doi.org/10.1016/S1387-1811(98)00257-1.
[96] L. Xiao, J. Li, H. Jin, R. Xu, Removal of organic templates from mesoporous SBA-15 at room temperature using UV/dilute H2O2, Microporous Mesoporous Mater. 96 (2006) 413–418, https://doi.org/10.1016/j.micromeso.2006.07.019.
[97] A. Marcilla, M. Beltran, I. Martinez, D. Berenguer, Chemical Engineering Research and Design Template removal in MCM-41 type materials by solvent extraction Influence of the treatment on the textural properties of the material and the effect on its behaviour as catalyst for reducing tobacco smoking toxicit, Chem. Eng. Res. Des. 89 (2011) 2330–2343, https://doi.org/10.1016/j.cherd.2011.04.015.
[98] J.M. Kim, J.H. Kwak, S. Jun, R. Ryoo, Ion exchange and thermal stability of MCM-41, J. Phys. Chem. 99 (1995) 16742–16747, https://doi.org/10.1021/j100045a039.
[99] H.M. Mody, S. Kannan, H.C. Bajaj, V. Manu, R.V. Jasra, A simple room temperature synthesis of MCM-41 with enhanced thermal and hydrothermal stability, J. Porous Mater. 15 (2008) 571–579, https://doi.org/10.1007/s10934-007-9135-1.
[100] A. Corma, M.T. Navarro, J.P. Pariente, Synthesis of an ultralarge pore titanium silicate isomorphous to MCM-41 and its application as a catalyst for selective oxidation of hydrocarbons, J. Chem. Soc., Chem. Commun. (1994) 147–148, https://doi.org/10.1039/C39940000147.
[101] G.J. Wang, Y. Wang, Y. Liu, Z. Liu, Y.J. Guo, G. Liu, Z. Yang, M.X. Xu, L. Wang, Synthesis of highly regular mesoporous Al-MCM-41 from metakaolin, Appl. Clay Sci. 44 (2009) 185–188, https://doi.org/10.1016/j.clay.2008.12.002.
[102] C. Siriluk, S. Yuttapong, Structure of mesoporous MCM-41 prepared from rice husk ash, 8Th Asian Symp. Vis. 2005, 2005, p. 7.
[103] V. Sanhueza, L. López-Escobar, U. Kelm, R. Cid, Synthesis of a mesoporous material from two natural sources, J. Chem. Technol. Biotechnol. 81 (2006) 614–617, https://doi.org/10.1002/jctb.1443.
[104] E. Du, S. Yu, L. Zuo, J. Zhang, X. Huang, Y. Wang, Pb(II) sorption on molecular sieve analogues of MCM-41 synthesized from kaolinite and montmorillonite, Appl. Clay Sci. 51 (2011) 94–101 https://doi.org/10.1016/j.clay.2010.11.009.
[105] T. Jiang, L. Qi, M. Ji, H. Ding, Y. Li, Z. Tao, Q. Zhao, Characterization of Y/MCM-41 composite molecular sieve with high stability from Kaolin and its catalytic property, Appl. Clay Sci. 62–63 (2012) 32–40 https://doi.org/10.1016/j.clay.2012.04.016.
[106] A. Glotov, N. Levshakov, A. Stavitskaya, M. Artemova, P. Gushchin, E. Ivanov, V. Vinokurov, Y. Lvov, Templated self-assembly of ordered mesoporous silica on clay nanotubes, Chem. Commun. 55 (2019) 5507–5510, https://doi.org/10.1039/c9cc01935a.
[107] J.A.S. Costa, C.M. Paranhos, Systematic evaluation of amorphous silica production from rice husk ashes, J. Clean. Prod. 192 (2018) 688–697, https://doi.org/10.1016/j.jclepro.2018.05.028.
[108] T. Yokoi, T. Tatsumi, Synthesis of mesoporous silica materials by using anionic surfactants as template, J. Jpn. Pet. Inst. 50 (2008) 299–311, https://doi.org/10.1627/jpi.50.299.
[109] Z. Wang, Y. Jiang, R. Rachwalik, Z. Liu, J. Shi, M. Hunger, J. Huang, One-step room-temperature synthesis of [Al]MCM-41 materials for the catalytic conversion of phenylglyoxal to ethylmandelate, ChemCatChem 5 (2013) 3889–3896, https://doi.org/10.1002/cctc.201300375.
[110] J.W. Park, D.S. Jung, M.E. Seo, S.Y. Kim, W.-J. Moon, C.-H. Shin, G. Seo, Preparation of mesoporous materials with adjustable pore size using anionic and cationic surfactants, Microporous Mesoporous Mater. 112 (2008) 458–466, https://doi.org/10.1016/j.micromeso.2007.10.023.
[111] J. Brown, R. Richer, L. Mercier, One-step synthesis of high capacity mesoporous Hg2+ adsorbents by non-ionic surfactant assembly, Microporous Mesoporous Mater. 37 (2000) 41–48 https://doi.org/10.1016/S1387-1811(99)00191-2.
[112] A. Léonard, J.L. Blin, P.A. Jacobs, P. Grange, B.L. Su, Chemistry of silica at different concentrations of non-ionic surfactant solutions: effect of pH of the synthesis gel on the preparation of mesoporous silicas, Microporous Mesoporous Mater. 63 (2003) 59–73, https://doi.org/10.1016/S1387-1811(03)00432-3.
[113] F. Chen, L. Huang, X. Yang, Z. Wang, Synthesis of Al-substituted MCM-41 and MCM-48 solid acids with mixed cationic–anionic surfactants as templates, Mater. Lett. 109 (2013) 299–301, https://doi.org/10.1016/j.matlet.2013.07.079.
[114] L.B. McCusker, C. Baerlocher, E. Jahn, M. Bülow, The triple helix inside the large-pore aluminophosphate molecular sieve VPI-5, Zeolites 11 (1991) 308–313 https://doi.org/10.1016/0144-2449(91)80292-8.
[115] P.T. Tanev, T.J. Pinnavaia, A neutral templating route to mesoporous molecular sieves, 80-, Science (1995) 267, https://doi.org/10.1126/science.267.5199.865 865 LP – 867.
[116] Y. Wei, J. Xu, Q. Feng, H. Dong, M. Lin, Encapsulation of enzymes in mesoporous host materials via the nonsurfactant-templated sol–gel process, Mater. Lett. 44 (2000) 6–11 https://doi.org/10.1016/S0167-577X(99)00287-6.
[117] Y. Wei, J. Xu, Q. Feng, M. Lin, H. Dong, W.J. Zhang, C. Wang, A novel method for enzyme immobilization: direct encapsulation of acid phosphatase in nanoporous silica host materials, J. Nanosci. Nanotechnol. 1 (2001) 83–93.
[118] P.M. Price, J.H. Clark, D.J. Macquarrie, Modified silicas for clean technology, J. Chem. Soc. Dalton Trans. (2000) 101–110, https://doi.org/10.1039/a905457j.
[119] S.L. Burkett, S.D. Sims, S. Mann, Synthesis of hybrid inorganic-organic mesoporous silica by co-condensation of siloxane and organosiloxane precursors, Chem. Commun. 0 (1996) 1367–1368, https://doi.org/10.1039/CC9960001367.
[120] H. Yang, N. Coombs, G.A. Ozin, Morphogenesis of shapes and surface patterns in mesoporous silica, Nature 386 (1997) 692–695, https://doi.org/10.1038/386692a0.
[121] S. Ahmed, A. Ramli, S. Yusup, Development of polyethylenimine-functionalized mesoporous Si-MCM-41 for CO2adsorption, Fuel Process. Technol. 167 (2017) 622–630, https://doi.org/10.1016/j.fuproc.2017.07.036.
[122] D.T. On, D. Desplantier-Giscard, C. Danumah, S. Kaliaguine, Perspectives in catalytic applications of mesostructured materials, Appl. Catal. Gen. 222 (2001) 299–357.
[123] M. Selvaraj, P.K. Sinha, K. Lee, I. Ahn, A. Pandurangan, T.G. Lee, Synthesis and characterization of Mn-MCM-41 and Zr-Mn-MCM-41, Microporous Mesoporous Mater. 78 (2005) 139–149, https://doi.org/10.1016/j.micromeso.2004.10.004.
[124] B. Boukoussa, R. Hamacha, A. Morsli, A. Bengueddach, Adsorption of yellow dye on calcined or uncalcined Al-MCM-41 mesoporous materials, Arab. J. Chem. 10 (2017) S2160–S2169, https://doi.org/10.1016/j.arabjc.2013.07.049.
[125] A.N. Gleizes, A. Fernandes, J. Dexpert-Ghys, Grafting 4f and 3d metal complexes into mesoporous MCM-41 silica by wet impregnation and by chemical vapour infiltration, J. Alloy. Comp. 374 (2004) 303–306, https://doi.org/10.1016/j.jallcom.2003.11.128.
[126] F.A.C. Garcia, V.S. Braga, J.C.M. Silva, J.A. Dias, S.C.L. Dias, J.L.B. Davo, Acidic characterization of copper oxide and niobium pentoxide supported on silica-alumina, Catal. Lett. 119 (2007) 101–107, https://doi.org/10.1007/s10562-007-9204-8.
[127] R. Soltani, M. Dinari, G. Mohammadnezhad, Ultrasonic-assisted synthesis of novel nanocomposite of poly(vinyl alcohol) and amino-modified MCM-41: a green adsorbent for Cd(II) removal, Ultrason. Sonochem. 40 (2018) 533–542, https://doi.org/10.1016/j.ultsonch.2017.07.045.
[128] A.A. Christy, Effect of hydrothermal treatment on adsorption properties of silica gel, Ind. Eng. Chem. Res. 50 (2011) 5543–5549, https://doi.org/10.1021/ie1018468.
[129] P. Kumar, V.V. Guliants, Periodic mesoporous organic-inorganic hybrid materials: applications in membrane separations and adsorption, Microporous Mesoporous Mater. 132 (2010) 1–14, https://doi.org/10.1016/j.micromeso.2010.02.007.
[130] S.J. Park, S.Y. Lee, A study on hydrogen-storage behaviors of nickel-loaded mesoporous MCM-41, J. Colloid Interface Sci. 346 (2010) 194–198, https://doi.org/10.1016/j.jcis.2010.02.047.
[131] S. Ahmed, A. Ramli, S. Yusup, CO2 adsorption study on primary, secondary and tertiary amine functionalized Si-MCM-41, Int. J. Greenh. Gas Control 51 (2016) 230–238, https://doi.org/10.1016/j.ijggc.2016.05.021.
[132] F. Adam, C.W. Kueh, Heterogeneous para-phenylamino sulfonic acid ligand functionalizedon MCM-41 derived from rice husk ash: selective mono-alkylated-products of tert-butylation of phenol, Appl. Catal. Gen. 489 (2015) 162–170, https://doi.org/10.1016/j.apcata.2014.09.047.
[133] S. Ahmed, A. Ramli, S. Yusup, M. Farooq, Adsorption behavior of tetraethylenepentamine-functionalized Si-MCM-41 for CO2 adsorption, Chem. Eng. Res. Des. 122 (2017) 33–42.
[134] J.N. Appaturi, M. Selvaraj, S.B. Abdul Hamid, M.R. Bin Johan, Synthesis of 3-(2-furylmethylene)-2,4-pentanedione using DL-Alanine functionalized MCM-41 catalyst via Knoevenagel condensation reaction, Microporous Mesoporous Mater. 260 (2018) 260–269, https://doi.org/10.1016/j.micromeso.2017.03.031.
[135] C.O. Arean, M.J. Vesga, J.B. Parra, M.R. Delgado, Effect of amine and carboxyl functionalization of sub-micrometric MCM-41 spheres on controlled release of cisplatin, Ceram. Int. 39 (2013) 7407–7414, https://doi.org/10.1016/j.ceramint.2013.02.084.
[136] G. Berlier, L. Gastaldi, E. Ugazio, I. Miletto, P. Iliade, S. Sapino, Stabilization of quercetin flavonoid in MCM-41 mesoporous silica: positive effect of surface functionalization, J. Colloid Interface Sci. 393 (2013) 109–118, https://doi.org/10.1016/j.jcis.2012.10.073.
[137] M.L. Cerrada, A. Bento, E. Pérez, V. Lorenzo, J.P. Lourenço, M.R. Ribeiro, Hybrid materials based on polyethylene and MCM-41 microparticles functionalized with silanes: catalytic aspects of in situ polymerization, crystalline features and mechanical properties, Microporous Mesoporous Mater. 232 (2016) 86–96, https://doi.org/10.1016/j.micromeso.2016.06.011.
[138] Y. Fazaeli, S. Feizi, A.R. Jalilian, A. Hejrani, Grafting of [64Cu]-TPPF20porphyrin complex on Functionalized nano-porous MCM-41 silica as a potential cancer imaging agent, Appl. Radiat. Isot. 112 (2016) 13–19, https://doi.org/10.1016/j.apradiso.2016.03.003.

[139] N. Fellenz, F.J. Perez-Alonso, P.P. Martin, J.L. García-Fierro, J.F. Bengoa, S.G. Marchetti, S. Rojas, Chromium (VI) removal from water by means of adsorption-reduction at the surface of amino-functionalized MCM-41 sorbents, Microporous Mesoporous Mater. 239 (2017) 138–146, https://doi.org/10.1016/j.micromeso.2016.10.012.
[140] Y. Guo, D. Liu, Y. Zhao, B. Gong, Y. Guo, W. Huang, Synthesis of chitosan-functionalized MCM-41-A and its performance in Pb(II) removal from synthetic water, J. Taiwan Inst. Chem. Eng. 71 (2017) 537–545.
[141] W. Hao, G. Ding, M. Cai, A phosphine-free heterogeneous formylation of aryl halides catalyzed by a thioether-functionalized MCM-41-immobilized palladium complex, Catal. Commun. 51 (2014) 53–57, https://doi.org/10.1016/j.catcom.2014.03.027.
[142] H.M.A. Hassan, E.M. Saad, M.S. Soltan, M.A. Betiha, I.S. Butler, S.I. Mostafa, A palladium(II) 4-hydroxysalicylidene Schiff-base complex anchored on functionalized MCM-41: an efficient heterogeneous catalyst for the epoxidation of olefins, Appl. Catal. Gen. 488 (2014) 148–159, https://doi.org/10.1016/j.apcata.2014.09.040.
[143] R. Hu, L. Zha, M. Cai, MCM-41-supported mercapto platinum complex as a highly efficient catalyst for the hydrosilylation of olefins with triethoxysilane, Catal. Commun. 11 (2010) 563–566, https://doi.org/10.1016/j.catcom.2009.12.020.
[144] S.A. Idris, S.R. Harvey, L.T. Gibson, Selective extraction of mercury(II) from water samples using mercapto functionalised-MCM-41 and regeneration of the sorbent using microwave digestion, J. Hazard Mater. 193 (2011) 171–176, https://doi.org/10.1016/j.jhazmat.2011.07.037.
[145] A.L. Khan, C. Klaysom, A. Gahlaut, A.U. Khan, I.F.J. Vankelecom, Mixed matrix membranes comprising of Matrimid and -SO3H functionalized mesoporous MCM-41 for gas separation, J. Membr. Sci. 447 (2013) 73–79, https://doi.org/10.1016/j.memsci.2013.07.011.
[146] K. Kermannezhad, A. Najafi Chermahini, M.M. Momeni, B. Rezaei, Application of amine-functionalized MCM-41 as pH-sensitive nano container for controlled release of 2-mercaptobenzoxazole corrosion inhibitor, Chem. Eng. J. 306 (2016) 849–857, https://doi.org/10.1016/j.cej.2016.08.004.
[147] A.L. Khan, C. Klaysom, A. Gahlaut, I.F.J. Vankelecom, Polysulfone acrylate membranes containing functionalized mesoporous MCM-41 for CO 2 separation, J. Membr. Sci. 436 (2013) 145–153, https://doi.org/10.1016/j.memsci.2013.02.023.
[148] W.Z. Lang, X.W. Liu, Y.J. Guo, B. Su, L.F. Chu, C.X. Guo, A novel MCM-41-supported bi-functional catalyst by immobilizing organoamine and Rh-P complex for one-pot synthesis of 2-ethylhexenal from propene, Microporous Mesoporous Mater. 142 (2011) 7–16, https://doi.org/10.1016/j.micromeso.2010.07.019.
[149] Y.L. Lau, Y.F. Yeong, Optimization of nitrate removal from aqueous solution by amine-functionalized MCM-41 using response surface methodology, Procedia Eng 148 (2016) 1239–1246, https://doi.org/10.1016/j.proeng.2016.06.485.
[150] Y. Li, B. Yan, Lanthanide (Tb3+, Eu3+) functionalized MCM-41 through modified meta-aminobenzoic acid linkage: covalently bonding assembly, physical characterization and photoluminescence, Microporous Mesoporous Mater. 128 (2010) 62–70, https://doi.org/10.1016/j.micromeso.2009.08.005.
[151] G. Luo, L. Kang, M. Zhu, B. Dai, Highly active phosphotungstic acid immobilized on amino functionalized MCM-41 for the oxidesulfurization of dibenzothiophene, Fuel Process. Technol. 118 (2014) 20–27, https://doi.org/10.1016/j.fuproc.2013.08.001.
[152] G. Maria, A.I. Stoica, I. Luta, D. Stirbet, G.L. Radu, Cephalosporin release from functionalized MCM-41 supports interpreted by various models, Microporous Mesoporous Mater. 162 (2012) 80–90, https://doi.org/10.1016/j.micromeso.2012.06.013.
[153] A. Mathew, S. Parambadath, M.J. Barnabas, H.J. Song, J.S. Kim, S.S. Park, C.S. Ha, Rhodamine 6G assisted adsorption of metanil yellow over succinamic acid functionalized MCM-41, Dyes Pigments 131 (2016) 177–185, https://doi.org/10.1016/j.dyepig.2016.04.007.
[154] R.D.S. Oliveira, F.F. Camilo, M.A. Bizeto, Evaluation of the influence of sulfur-based functional groups on the embedding of silver nanoparticles into the pores of MCM-41, J. Solid State Chem. 235 (2016) 125–131, https://doi.org/10.1016/j.jssc.2015.12.024.
[155] S. Parambadath, A. Mathew, S.S. Park, C.S. Ha, Pentane-1,2-dicarboxylic acid functionalized spherical MCM-41: a simple and highly selective heterogeneous ligand for the adsorption of Fe^{3+} from aqueous solutions, J. Environ. Chem. Eng. 3 (2015) 1918–1927, https://doi.org/10.1016/j.jece.2015.07.003.
[156] N.N. Pesyan, H. Batmani, F. Havasi, Copper supported on functionalized MCM-41 as a novel and a powerful heterogeneous nanocatalyst for the synthesis of benzothiazoles, Polyhedron 158 (2019) 248–254, https://doi.org/10.1016/j.poly.2018.11.005.
[157] M. Rafiee, B. Karimi, S. Farrokhzadeh, H. Vali, Hydroquinone functionalized oriented MCM-41 mesochannels at the electrode surface, Electrochim. Acta 94 (2013) 198–205, https://doi.org/10.1016/j.electacta.2013.01.147.
[158] V. Rizzi, E.A. Prasetyanto, P. Chen, J. Gubitosa, P. Fini, A. Agostiano, L. De Cola, P. Cosma, Amino grafted MCM-41 as highly efficient and reversible ecofriendly adsorbent material for the Direct Blue removal from wastewater, J. Mol. Liq. 273 (2019) 435–446, https://doi.org/10.1016/j.molliq.2018.10.060.
[159] M. Sadeghi, S. Yekta, H. Ghaedi, Synthesis and application of Pb-MCM-41/ZnNiO2 as a novel mesoporous nanocomposite adsorbent for the decontamination of chloroethyl phenyl sulfide (CEPS), Appl. Surf. Sci. 400 (2017) 471–480, https://doi.org/10.1016/j.apsusc.2016.12.224.
[160] R. Sanz, G. Calleja, A. Arencibia, E.S. Sanz-Pérez, CO2 capture with pore-expanded MCM-41 silica modified with amino groups by double functionalization, Microporous Mesoporous Mater. 209 (2015) 165–171, https://doi.org/10.1016/j.micromeso.2014.10.045.
[161] X. Sheng, J. Gao, L. Han, Y. Jia, W. Sheng, One-pot synthesis of tryptophols with mesoporous MCM-41 silica catalyst functionalized with sulfonic acid groups, Microporous Mesoporous Mater. 143 (2011) 73–77, https://doi.org/10.1016/j.micromeso.2011.02.008.
[162] P. Solanki, S. Patel, R. Devkar, A. Patel, Camptothecin encapsulated into functionalized MCM-41: in vitro release study, cytotoxicity and kinetics, Mater. Sci. Eng. C 98 (2019) 1014–1021, https://doi.org/10.1016/j.msec.2019.01.065.
[163] A. Ulu, I. Ozcan, S. Koytepe, B. Ates, Design of epoxy-functionalized Fe3O4@MCM-41 core–shell nanoparticles for enzyme immobilization, Int. J. Biol. Macromol. 115 (2018) 1122–1130, https://doi.org/10.1016/j.ijbiomac.2016.12.051.
[164] H. Wu, X. Li, Y. Li, S. Wang, R. Guo, Z. Jiang, C. Wu, Q. Xin, X. Lu, Facilitated transport mixed matrix membranes incorporated with amine functionalized MCM-41 for enhanced gas separation properties, J. Membr. Sci. 465 (2014) 78–90, https://doi.org/10.1016/j.memsci.2014.04.023.
[165] D. Xie, Q. He, Y. Su, T. Wang, R. Xu, B. Hu, Oxidative desulfurization of dibenzothiophene catalyzed by peroxotungstate on functionalized MCM-41 materials using hydrogen peroxide as oxidant, Cuihua Xuebao/Chinese J. Catal. 36 (2015) 1205–1213, https://doi.org/10.1016/S1872-2067(15)60897-X.
[166] F. Yang, S. Gao, C. Xiong, H. Wang, J. Chen, Y. Kong, Coordination of manganese porphyrins on amino-functionalized MCM-41 for heterogeneous catalysis of naphthalene hydroxylation, Cuihua Xuebao/Chinese J. Catal. 36 (2015) 1035–1041, https://doi.org/10.1016/S1872-2067(15)60836-1.
[167] L.F. Zha, W. Sen Yang, W.Y. Hao, M.Z. Cai, Hydrosilylation of olefins over rhodium complex anchored over thioether-functionalized MCM-41, Chin. Chem. Lett. 21 (2010) 1310–1313, https://doi.org/10.1016/j.cclet.2010.06.007.
[168] J. Zhang, G. Huang, C. Zhang, Q. He, C. Huang, X. Yang, H. Song, Z. Liang, L. Du, S. Liao, Immobilization of highly active Pd nano-catalysts on functionalized mesoporous silica supports using mercapto groups as anchoring sites and their catalytic performance for phenol hydrogenation, Cuihua Xuebao/Chinese J. Catal. 34 (2013) 1519–1526, https://doi.org/10.1016/S1872-2067(12)60603-2.
[169] M. Zhang, W. Zhu, H. Li, S. Xun, W. Ding, J. Liu, Z. Zhao, Q. Wang, One-pot synthesis, characterization and desulfurization of functional mesoporous W-MCM-41 from POM-based ionic liquids, Chem. Eng. J. 243 (2014) 386–393, https://doi.org/10.1016/j.cej.2013.12.093.
[170] J.A.S. Costa, R.A. de Jesus, D.D. Dorst, I.M. Pinatti, L.M.R. Oliveira, M.E. de Mesquita, C.M. Paranhos, Photoluminescent properties of the europium and terbium complexes covalently bonded to functionalized mesoporous material PABA-MCM-41, J. Lumin. 192 (2017) 1149–1156, https://doi.org/10.1016/j.jlumin.2017.08.046.
[171] I.P. de Sá, J.M. Higuera, V.C. Costa, J.A.S. Costa, C.M.P. da Silva, A.R.A. Nogueira, Determination of trace elements in meat and fish samples by MIP OES using solid-phase extraction, Food Anal. Methods. (2019), https://doi.org/10.1007/s12161-019-01615-3.
[172] J.A. Wang, L.F. Chen, L.E. Noreña, J. Navarrete, M.E. Llanos, J.L. Contreras, O. Novaro, Mesoporous structure, surface acidity and catalytic properties of Pt/Zr-MCM-41 catalysts promoted with 12-tungstophosphoric acid, Microporous Mesoporous Mater. 112 (2008) 61–76, https://doi.org/10.1016/j.micromeso.2007.09.015.
[173] I. Mandache, V.I. Parvulescu, A. Popescu, L. Pârvulescu, M.D. Banciu, P. Amoros, D. Beltran, D.T. On, S. Kaliaguine, Epoxidation of dibenzocycloalkenes on Ti-Ge-MCM-41 and Ti-SBA-15 catalysts, Microporous Mesoporous Mater. 81 (2005) 115–124, https://doi.org/10.1016/j.micromeso.2005.01.024.
[174] M. Fadhli, I. Khedher, J.M. Fraile, Modified Ti/MCM-41 catalysts for enantioselective epoxidation of styrene, J. Mol. Catal. A Chem. 420 (2016) 282–289, https://doi.org/10.1016/j.molcata.2016.05.001.
[175] E.R. Naranov, A.A. Sadovnikov, A.L. Maximov, E.A. Karakhanov, Development of micro-mesoporous materials with lamellar structure as the support of NiW catalysts, Microporous Mesoporous Mater. 263 (2018) 150–157, https://doi.org/10.1016/j.micromeso.2017.12.021.
[176] A. Glotov, N. Levshakov, A. Vutolkina, S. Lysenko, E. Karakhanov, V. Vinokurov, Aluminosilicates supported La-containing sulfur reduction additives for FCC catalyst: correlation between activity, support structure and acidity, Catal. Today 329 (2019) 135–141, https://doi.org/10.1016/j.cattod.2018.10.009.
[177] A.V. Vutolkina, A.P. Glotov, A.V. Zanina, D.F. Makhmutov, A.L. Maximov, S.V. Egazar'yants, E.A. Karakhanov, Mesoporous Al-HMS and Al-MCM-41 supported Ni-Mo sulfide catalysts for HYD and HDS via in situ hydrogen generation through a WGSR, Catal. Today 329 (2019) 156–166, https://doi.org/10.1016/j.cattod.2018.11.030.
[178] Y.V. Patrushev, V.N. Sidelnikov, The properties of capillary columns with silica organic-inorganic MCM-41 type porous layer stationary phase, J. Chromatogr., A 1351 (2014) 103–109, https://doi.org/10.1016/j.chroma.2014.05.042.
[179] Z. Li, A.J. González, V.B. Heeralal, D.Y. Wang, Covalent assembly of MCM-41 nanospheres on graphene oxide for improving fire retardancy and mechanical property of epoxy resin, Compos. B Eng. 138 (2018) 101–112, https://doi.org/10.1016/j.compositesb.2017.11.001.
[180] A. Woszuk, R. Panek, J. Madej, A. Zofka, W. Franus, Mesoporous silica material MCM-41: novel additive for warm mix asphalts, Constr. Build. Mater. 183 (2018) 270–274, https://doi.org/10.1016/j.conbuildmat.2018.06.177.
[181] R. Mortera, B. Onida, S. Fiorilli, V. Cauda, C.V. Brovarone, F. Baino, E. Vernè, E. Garrone, Synthesis and characterization of MCM-41 spheres inside bioactive glass-ceramic scaffold, Chem. Eng. J. 137 (2008) 54–61, https://doi.org/10.1016/j.cej.2007.07.094.
[182] N. Lakshminarasimman, O. Quiñones, B.J. Vanderford, P. Campo-Moreno, E.V. Dickenson, D.C. McAvoy, Biotransformation and sorption of trace organic compounds in biological nutrient removal treatment systems, Sci. Total Environ.

640–641 (2018) 62–72, https://doi.org/10.1016/J.SCITOTENV.2018.05.145.
[183] C. Bertoldi, A.G. Rodrigues, A.N. Fernandes, Removal of endocrine disrupters in water under artificial light: the effect of organic matter, J. Water Process Eng. 27 (2019) 126–133, https://doi.org/10.1016/j.jwpe.2018.11.016.
[184] A. Abdelrady, S. Sharma, A. Sefelnasr, A. Abogbal, M. Kennedy, Investigating the impact of temperature and organic matter on the removal of selected organic micropollutants during bank filtration: a batch study, J. Environ. Chem. Eng. 7 (2019) 102904, https://doi.org/10.1016/J.JECE.2019.102904.
[185] J. Kujawa, S. Cerneaux, W. Kujawski, Highly hydrophobic ceramic membranes applied to the removal of volatile organic compounds in pervaporation, Chem. Eng. J. 260 (2015) 43–54, https://doi.org/10.1016/J.CEJ.2014.08.092.
[186] X. Si, Z. Hu, D. Ding, X. Fu, Effects of effluent organic matters on endocrine disrupting chemical removal by ultrafiltration and ozonation in synthetic secondary effluent, J. Environ. Sci. 76 (2019) 57–64, https://doi.org/10.1016/J.JES.2018.03.025.
[187] J. Müller, K.S. Jewell, M. Schulz, N. Hermes, T.A. Ternes, J.E. Drewes, U. Hübner, Capturing the oxic transformation of iopromide – a useful tool for an improved characterization of predominant redox conditions and the removal of trace organic compounds in biofiltration systems? Water Res. 152 (2019) 274–284, https://doi.org/10.1016/J.WATRES.2018.12.055.
[188] M.J. McKie, M.C. Ziv-El, L. Taylor-Edmonds, R.C. Andrews, M.J. Kirisits, Biofilter scaling procedures for organics removal: a potential alternative to piloting, Water Res. 151 (2019) 87–97, https://doi.org/10.1016/J.WATRES.2018.12.006.
[189] M.A. Al-Obaidi, C. Kara-Zaïtri, I.M. Mujtaba, Simultaneous removal of organic compounds from wastewater using reverse osmosis process: modelling, simulation, and optimisation, Comput. Aided Chem. Eng. 44 (2018) 1867–1872, https://doi.org/10.1016/B978-0-444-64241-7.50306-2.
[190] H.N. Altalyan, B. Jones, J. Bradd, L.D. Nghiem, Y.M. Alyazichi, Removal of volatile organic compounds (VOCs) from groundwater by reverse osmosis and nanofiltration, J. Water Process Eng. 9 (2016) 9–21, https://doi.org/10.1016/J.JWPE.2015.11.010.
[191] N. Wang, Z. Xu, W. Xu, J. Xu, Y. Chen, M. Zhang, Comparison of coagulation and magnetic chitosan nanoparticle adsorption on the removals of organic compound and coexisting humic acid: a case study with salicylic acid, Chem. Eng. J. 347 (2018) 514–524, https://doi.org/10.1016/J.CEJ.2018.04.131.
[192] J.S. Rosenblum, K.A. Sitterley, E.M. Thurman, I. Ferrer, K.G. Linden, Hydraulic fracturing wastewater treatment by coagulation-adsorption for removal of organic compounds and turbidity, J. Environ. Chem. Eng. 4 (2016) 1978–1984, https://doi.org/10.1016/J.JECE.2016.03.013.
[193] M.F. Mustafa, X. Fu, Y. Liu, Y. Abbas, H. Wang, W. Lu, Volatile organic compounds (VOCs) removal in non-thermal plasma double dielectric barrier discharge reactor, J. Hazard Mater. 347 (2018) 317–324, https://doi.org/10.1016/J.JHAZMAT.2018.01.021.
[194] H. Wang, D. Heil, Z.J. Ren, P. Xu, Removal and fate of trace organic compounds in microbial fuel cells, Chemosphere 125 (2015) 94–101, https://doi.org/10.1016/J.CHEMOSPHERE.2014.11.048.
[195] C.M. López-Ortiz, I. Sentana-Gadea, P.J. Varó-Galvañ, S.E. Maestre-Pérez, D. Prats-Rico, Effect of magnetic ion exchange (MIEX®) on removal of emerging organic contaminants, Chemosphere 208 (2018) 433–440, https://doi.org/10.1016/J.CHEMOSPHERE.2018.05.194.
[196] M.M. Hamed, M. Holiel, Y.F. El-Aryan, Removal of selenium and iodine radionuclides from waste solutions using synthetic inorganic ion exchanger, J. Mol. Liq. 242 (2017) 722–731, https://doi.org/10.1016/J.MOLLIQ.2017.07.035.
[197] C. Cameselle, S. Gouveia, Electrokinetic remediation for the removal of organic contaminants in soils, Curr. Opin. Electrochem. 11 (2018) 41–47, https://doi.org/10.1016/J.COELEC.2018.07.005.
[198] S. Annamalai, M. Santhanam, M. Sundaram, M.P. Curras, Electrokinetic remediation of inorganic and organic pollutants in textile effluent contaminated agricultural soil, Chemosphere 117 (2014) 673–678, https://doi.org/10.1016/J.CHEMOSPHERE.2014.10.023.
[199] C. Onorato, L.J. Banasiak, A.I. Schäfer, Inorganic trace contaminant removal from real brackish groundwater using electrodialysis, Separ. Purif. Technol. 187 (2017) 426–435, https://doi.org/10.1016/J.SEPPUR.2017.06.016.
[200] A. Šuligoj, U.L. Štangar, A. Ristić, M. Mazaj, D. Verhovšek, N.N. Tušar, TiO2–SiO2 films from organic-free colloidal TiO2 anatase nanoparticles as photocatalyst for removal of volatile organic compounds from indoor air, Appl. Catal. B Environ. 184 (2016) 119–131, https://doi.org/10.1016/J.APCATB.2015.11.007.
[201] N. Berezina, B. Yada, R. Lefebvre, From organic pollutants to bioplastics: insights into the bioremediation of aromatic compounds by Cupriavidus necator, Nat. Biotechnol. 32 (2015) 47–53, https://doi.org/10.1016/J.NBT.2014.09.003.
[202] C.-F. Yang, S.-H. Liu, Y.-M. Su, Y.-R. Chen, C.-W. Lin, K.-L. Lin, Bioremediation capability evaluation of benzene and sulfolane contaminated groundwater: determination of bioremediation parameters, Sci. Total Environ. 648 (2019) 811–818, https://doi.org/10.1016/J.SCITOTENV.2018.08.208.
[203] X. Li, X. Wang, Y. Chen, X. Yang, Z. Cui, Optimization of combined phytoremediation for heavy metal contaminated mine tailings by a field-scale orthogonal experiment, Ecotoxicol. Environ. Saf. 168 (2019) 1–8, https://doi.org/10.1016/J.ECOENV.2018.10.012.
[204] W. Guidi Nissim, A. Cincinelli, T. Martellini, L. Alvisi, E. Palm, S. Mancuso, E. Azzarello, Phytoremediation of sewage sludge contaminated by trace elements and organic compounds, Environ. Res. 164 (2018) 356–366, https://doi.org/10.1016/J.ENVRES.2018.03.009.
[205] S.O. Akpotu, B. Moodley, Application of as-synthesised MCM-41 and MCM-41 wrapped with reduced graphene oxide/graphene oxide in the remediation of acetaminophen and aspirin from aqueous system, J. Environ. Manag. 209 (2018) 205–215, https://doi.org/10.1016/j.jenvman.2017.12.037.
[206] W. Chen, X. Li, Z. Pan, Y. Bao, S. Ma, L. Li, Efficient adsorption of Norfloxacin by Fe-MCM-41 molecular sieves: kinetic, isotherm and thermodynamic studies, Chem. Eng. J. 281 (2015) 397–403, https://doi.org/10.1016/j.cej.2015.06.121.
[207] J.A.S. Costa, C.M. Paranhos, Evaluation of rice husk ash in adsorption of Remazol Red dye from aqueous media, SN Appl. Sci. 1 (2019) 1–8, https://doi.org/10.1007/s42452-019-0436-1.
[208] R.S. Araújo, D.C.S. Azevedo, C.L. Cavalcante, A. Jiménez-Lopez, E. Rodrígues-Castellón, Adsorption of polycyclic aromatic hydrocarbons (PAHs) from isooctane solutions by mesoporous molecular sieves: influence of the surface acidity, Microporous Mesoporous Mater. 108 (2008) 213–222, https://doi.org/10.1016/j.micromeso.2007.04.005.
[209] Y. Hu, Y. He, X. Wang, C. Wei, Efficient adsorption of phenanthrene by simply synthesized hydrophobic MCM-41 molecular sieves, Appl. Surf. Sci. 311 (2014) 825–830, https://doi.org/10.1016/j.apsusc.2014.05.173.
[210] X. Yang, Q. Guan, W. Li, Effect of template in MCM-41 on the adsorption of aniline from aqueous solution, J. Environ. Manag. 92 (2011) 2939–2943, https://doi.org/10.1016/j.jenvman.2011.07.006.
[211] S.K. Toor, J.P. Kushwaha, V.K. Sangal, Adsorptive interaction of 4-aminobiphenyl with mesoporous MCM-41, Phys. Chem. Liq. 9104 (2018) 1–13, https://doi.org/10.1080/00319104.2018.1519564.
[212] C. Zhou, Q. Gao, W. Luo, Q. Zhou, H. Wang, C. Yan, Preparation, characterization and adsorption evaluation of spherical mesoporous Al-MCM-41 from coal fly ash, J. Taiwan Inst. Chem. Eng. 52 (2015) 147–157, https://doi.org/10.1016/j.jtice.2015.02.014.
[213] Y. Wu, M. Zhang, H. Zhao, S. Yang, A. Arkin, Functionalized mesoporous silica material and anionic dye adsorption: MCM-41 incorporated with amine groups for competitive adsorption of Acid Fuchsine and Acid Orange II, RSC Adv. 4 (2014) 61256–61267, https://doi.org/10.1039/c4ra11737a.
[214] Y. Shu, Y. Shao, X. Wei, X. Wang, Q. Sun, Q. Zhang, L. Li, Synthesis and characterization of Ni-MCM-41 for methyl blue adsorption, Microporous Mesoporous Mater. 214 (2015) 88–94, https://doi.org/10.1016/j.micromeso.2015.05.006.
[215] N. Gokulakrishnan, A. Pandurangan, P.K. Sinha, Removal of decontaminating agent ethylenediaminetetraacetic acid from aqueous solution by an effective mesoporous AI-MCM-41 molecular sieves adsorbent, Ind. Eng. Chem. Res. 45 (2006) 5326–5331, https://doi.org/10.1021/ie0511837.
[216] N. Gokulakrishnan, A. Pandurangan, T. Somanathan, P.K. Sinha, Uptake of decontaminating agent from aqueous solution: a study on adsorption behaviour of oxalic acid over Al-MCM-41 adsorbents, J. Porous Mater. 17 (2010) 763–771, https://doi.org/10.1007/s10934-009-9348-6.
[217] H. Sepehrian, J. Fasihi, M.K. Mahani, Adsorption behavior studies of picric acid on mesoporous MCM-41, Ind. Eng. Chem. Res. 48 (2009) 6772–6775, https://doi.org/10.1021/ie801716k.
[218] P. Gao, C. Yang, Z. Liang, W. Wang, Z. Zhao, B. Hu, F. Cui, N-propyl functionalized spherical mesoporous silica as a rapid and efficient adsorbent for steroid estrogen removal: adsorption behaviour and effects of water chemistry, Chemosphere 214 (2019) 361–370, https://doi.org/10.1016/j.chemosphere.2018.09.115.
[219] Y. Guo, W. Huang, B. Chen, Z. Ying, D. Liu, Y. Sun, B. Gong, Removal of tetracycline from aqueous solution by MCM-41-zeolite A loaded nano zero valent iron: synthesis, characteristic, adsorption performance and mechanism, J. Hazard Mater. 339 (2017) 22–32.
[220] M. Liu, L. an Hou, S. Yu, B. Xi, Y. Zhao, X. Xia, MCM-41 impregnated with A zeolite precursor: synthesis, characterization and tetracycline antibiotics removal from aqueous solution, Chem. Eng. J. 223 (2013) 678–687, https://doi.org/10.1016/j.cej.2013.02.088.
[221] K.Z. Hossain, C.M. Monreal, A. Sayari, Adsorption of urease on PE-MCM-41 and its catalytic effect on hydrolysis of urea, Colloids Surfaces B Biointerfaces 62 (2008) 42–50, https://doi.org/10.1016/j.colsurfb.2007.09.016.
[222] A. Katiyar, L. Ji, P.G. Smirniotis, N.G. Pinto, Adsorption of bovine serum albumin and lysozyme on siliceous MCM-41, Microporous Mesoporous Mater. 80 (2005) 311–320, https://doi.org/10.1016/j.micromeso.2004.11.026.
[223] X.Y. Sun, P.Z. Li, B. Ai, Y.B. Wang, Surface modification of MCM-41 and its application in DNA adsorption, Chin. Chem. Lett. 27 (2016) 139–144, https://doi.org/10.1016/j.cclet.2015.08.008.
[224] H. Tian, J. Li, L. Zou, Z. Mu, Z. Hao, Removal of DDT from aqueous solutions using mesoporous silica materials, J. Chem. Technol. Biotechnol. 84 (2009) 490–496, https://doi.org/10.1002/jctb.2067.
[225] M. Brigante, M. Avena, Synthesis, characterization and application of a hexagonal mesoporous silica for pesticide removal from aqueous solution, Microporous Mesoporous Mater. 191 (2014) 1–9, https://doi.org/10.1016/j.micromeso.2014.02.035.
[226] M.C. Bruzzoniti, R.M. de Carlo, C. Sarzanini, D. Caldarola, B. Onida, Novel insights in Al-MCM-41 precursor as adsorbent for regulated haloacetic acids and nitrate from water, Environ. Sci. Pollut. Res. 19 (2012) 4176–4183, https://doi.org/10.1007/s11356-012-0900-6.
[227] J.A.S. Costa, J.M. Santos, L.O. Dos Santos, I.C. Bellin, Extração e Caracterização de Substâncias Húmicas Aquáticas (SHA) Extraídas de Amostras Coletadas no Parque Nacional Serra de Itabaiana, Sergipe, Brasil, Rev. Ciências Ambient. 12 (2018) 7–23, https://doi.org/10.18316/rca.v12i3.2527.
[228] M. Ebrahimi-Gatkash, H. Younesi, A. Shahbazi, A. Heidari, Amino-functionalized mesoporous MCM-41 silica as an efficient adsorbent for water treatment: batch and fixed-bed column adsorption of the nitrate anion, Appl. Water Sci. 7 (2017) 1887–1901, https://doi.org/10.1007/s13201-015-0364-1.
[229] D. Li, H. Min, X. Jiang, X. Ran, L. Zou, J. Fan, One-pot synthesis of Aluminum-containing ordered mesoporous silica MCM-41 using coal fly ash for phosphate adsorption, J. Colloid Interface Sci. 404 (2013) 42–48, https://doi.org/10.1016/j.jcis.2013.04.018.

[230] M.K. Seliem, S. Komarneni, M.R. Abu Khadra, Phosphate removal from solution by composite of MCM-41 silica with rice husk: kinetic and equilibrium studies, Microporous Mesoporous Mater. 224 (2016) 51–57, https://doi.org/10.1016/j.micromeso.2015.11.011.
[231] J.A.S. Costa, V.H.V. Sarmento, L.P.C. Romão, Caio M. Paranhos, Synthesis of functionalized mesoporous material from rice husk ash and its application in the removal of the polycyclic aromatic hydrocarbons, Environ. Sci. Pollut. Res. (2019), https://doi.org/10.1007/s11356-019-05852-1.
[232] J.A.S. Costa, V.H.V. Sarmento, L.P.C. Romão, C.M.P. da Silva, Adsorption of organic compounds on mesoporous material from rice husk ash (RHA), Biomass Convers. Biorefinery. (2019), https://doi.org/10.1007/s13399-019-00476-4.
[233] X. Liu, Y. Hu, J. Huang, C. Wei, Detailed characteristics of adsorption of bisphenol A by highly hydrophobic MCM-41 mesoporous molecular sieves, Res. Chem. Intermed. 42 (2016) 7169–7183, https://doi.org/10.1007/s11164-016-2526-7.
[234] H. Xin, T. Ke, Preparation and adsorption denitrogenation from model fuel or diesel oil of heteroatoms mesoporous molecular sieve Co-MCM-41, Energy Sources, Part A Recover, Util. Environ. Eff. 38 (2016) 2560–2567, https://doi.org/10.1080/15567036.2015.1062823.
[235] E. Binaeian, H.A. Tayebi, A. Shokuhi Rad, S. Afrashteh, Adsorption of acid blue on synthesized polymeric nanocomposites, PPy/MCM-41 and PAni/MCM-41: isotherm, thermodynamic and kinetic studies, J. Macromol. Sci. Part A Pure Appl. Chem. 55 (2018) 269–279, https://doi.org/10.1080/10601325.2018.1424554.
[236] W.A. Talavera-Pech, A. Ávila-Ortega, D. Pacheco-Catalán, P. Quintana-Owen, J.A. Barrón-Zambrano, Effect of Functionalization Synthesis Type of Amino-MCM-41 Mesoporous Silica Nanoparticles on its RB5 Adsorption Capacity and Kinetics, Silicon, 2018.
[237] H. Chaudhuri, S. Dash, A. Sarkar, Adsorption of different dyes from aqueous solution using Si-MCM-41 having very high surface area, J. Porous Mater. 23 (2016) 1227–1237, https://doi.org/10.1007/s10934-016-0181-4.
[238] S.K. Hassaninejad-Darzi, H.Z. Mousavi, M. Ebrahimpour, Biosorption of Acridine Orange and Auramine O dyes onto MCM-41 mesoporous silica nanoparticles using high-accuracy UV–Vis partial least squares regression, J. Mol. Liq. 248 (2017) 990–1002, https://doi.org/10.1016/j.molliq.2017.10.126.
[239] B. Han, F. Zhang, Z. Feng, S. Liu, S. Deng, Y. Weng, Y. Wang, A designed Mn2O3/MCM-41 nanoporous composite for methylene blue and rhodamine B removal with high efficiency, Ceram. Int. 40 (2014) 8093–8101, https://doi.org/10.1016/j.ceramint.2013.12.163.
[240] T.A. Arica, E. Ayas, M.Y. Arica, Magnetic MCM-41 silica particles grafted with poly (glycidylmethacrylate) brush: modification and application for removal of direct dyes, Microporous Mesoporous Mater. 243 (2017) 164–175, https://doi.org/10.1016/j.micromeso.2017.02.011.
[241] G.E.D. Nascimento, M.M.M.B. Duarte, D.C.S. Sales, C.M.B.D.M. Barbosa, Kinetic and equilibrium adsorption studies for removal of naphthenic acids present in model mixture of aviation kerosene, Chem. Eng. Commun. 204 (2017) 105–110, https://doi.org/10.1080/00986445.2016.1241772.
[242] H.T. Teo, W.R. Siah, L. Yuliati, Enhanced adsorption of acetylsalicylic acid over hydrothermally synthesized iron oxide-mesoporous silica MCM-41 composites, J. Taiwan Inst. Chem. Eng. 65 (2016) 591–598, https://doi.org/10.1016/j.jtice.2016.06.006.
[243] M.A. Amani, A.M. Latifi, K. Tahvildari, R. Karimian, Removal of diazinon pesticide from aqueous solutions using MCM-41 type materials: isotherms, kinetics and thermodynamics, Int. J. Environ. Sci. Technol. 15 (2018) 1301–1312, https://doi.org/10.1007/s13762-017-1469-x.
[244] J.W. Choi, S.Y. Lee, S.G. Chung, S.W. Hong, D.J. Kim, S.H. Lee, Removal of phosphate from aqueous solution by functionalized mesoporous materials, Water Air Soil Pollut. 222 (2011) 243–254, https://doi.org/10.1007/s11270-011-0820-y.
[245] A. Kawasaki, S. Nishihama, K. Yoshizuka, Adsorption of tetraalkyl ammonium hydroxide with mesoporous silica, Separ. Sci. Technol. 47 (2012) 1356–1360, https://doi.org/10.1080/01496395.2012.672522.
[246] Q. Qin, Y. Xu, Enhanced nitrobenzene adsorption in aqueous solution by surface silylated MCM-41, Microporous Mesoporous Mater. 232 (2016) 143–150, https://doi.org/10.1016/j.micromeso.2016.06.018.
[247] Q. Qin, J. Ma, K. Liu, Adsorption of nitrobenzene from aqueous solution by MCM-41, J. Colloid Interface Sci. 315 (2007) 80–86, https://doi.org/10.1016/j.jcis.2007.06.060.
[248] K. Abbas, H. Znad, M.R. Awual, A ligand anchored conjugate adsorbent for effective mercury(II) detection and removal from aqueous media, Chem. Eng. J. 334 (2018) 432–443, https://doi.org/10.1016/j.cej.2017.10.054.
[249] K. Alizadeh, E. Khaledyan, Y. Mansourpanah, Synthesis and application of amin-modified Fe3O4@MCM-41 core-shell magnetic mesoporous for effective removal of pb2+ ions from aqueous solutions and optimization with response surface methodology, J. Water Environ. Nanotechnol. 3 (2018) 243–253, https://doi.org/10.22090/jwent.2018.03.005.
[250] Z. Hu, X. Zhang, D. Zhang, J.X. Wang, Adsorption of Cu2+ on amine-functionalized mesoporous silica brackets, Water Air Soil Pollut. 223 (2012) 2743–2749, https://doi.org/10.1007/s11270-011-1063-7.
[251] H.R.L.Z. Zhad, O. Sadeghi, M.M. Amini, N. Tavassoli, M.H. Banitaba, S.S.H. Davarani, Extraction of ultra trace amounts of palladium on 9-acridinylamine functionalized SBA-15 and MCM-41 nanoporous silica sorbents, Separ. Sci. Technol. 46 (2011) 648–655, https://doi.org/10.1080/01496395.2010.528501.
[252] R. He, Z. Wang, L. Tan, Y. Zhong, W. Li, D. Xing, C. Wei, Y. Tang, Design and fabrication of highly ordered ion imprinted SBA-15 and MCM-41 mesoporous organosilicas for efficient removal of Ni2+from different properties of wastewaters, Microporous Mesoporous Mater. 257 (2018) 212–221, https://doi.org/10.1016/j.micromeso.2017.08.007.
[253] J. Cao, Y. Wu, Y. Jin, P. Yilihan, W. Huang, Response surface methodology approach for optimization of the removal of chromium (VI) by NH2-MCM-41, J. Taiwan Inst. Chem. Eng. 45 (2014) 860–868, https://doi.org/10.1016/j.jtice.2013.09.011.
[254] H. Boojari, M. Pourafshari Chenar, M. Pakizeh, Experimental investigation of arsenic (III, V) removal from aqueous solution using synthesized α-Fe2O3/MCM-41 nanocomposite adsorbent, water, Air. Soil Pollut. 227 (2016), https://doi.org/10.1007/s11270-016-2989-6.
[255] A. Benhamou, J.P. Basly, M. Baudu, Z. Derriche, R. Hamacha, Amino-functionalized MCM-41 and MCM-48 for the removal of chromate and arsenate, J. Colloid Interface Sci. 404 (2013) 135–139, https://doi.org/10.1016/j.jcis.2013.04.026.
[256] Ş. Sert, M. Eral, Uranium adsorption studies on aminopropyl modified mesoporous sorbent (NH2-MCM-41) using statistical design method, J. Nucl. Mater. 406 (2010) 285–292, https://doi.org/10.1016/j.jnucmat.2010.08.024.
[257] F. Chen, M. Hong, W. You, C. Li, Y. Yu, Simultaneous efficient adsorption of Pb2+ and MnO4- ions by MCM-41 functionalized with amine and nitrilotriacetic acid anhydride, Appl. Surf. Sci. 357 (2015) 856–865, https://doi.org/10.1016/j.apsusc.2015.09.069.
[258] M.R. El-Naggar, R.F. Aglan, M.S. Sayed, Direct incorporation method for the synthesis of molybdophosphate/MCM-41 silica composite : adsorption study of heavy metals from aqueous solutions, J. Environ. Chem. Eng. 1 (2013) 516–525, https://doi.org/10.1016/j.jece.2013.06.026.
[259] H. Javadian, M. Taghavi, Application of novel Polypyrrole/thiol-functionalized zeolite Beta/MCM-41 type mesoporous silica nanocomposite for adsorption of Hg2+ from aqueous solution and industrial wastewater_/Kinetic, isotherm and thermodynamic studies, Appl. Surf. Sci. 289 (2014) 487–494.
[260] Y. Fu, Y. Huang, J. Hu, Preparation of chitosan/MCM-41-PAA nanocomposites and the adsorption behaviour of Hg(II) ions, R. Soc. Open Sci. 5 (2018) 1–12.
[261] D.F. Enache, E. Vasile, C.M. Simonescu, D. Culita, E. Vasile, O. Oprea, A.M. Pandele, A. Razvan, F. Dumitru, G. Nechifor, Schiff base-functionalized mesoporous silicas (MCM-41, HMS) as Pb(ii) adsorbents, RSC Adv. 8 (2018) 176–189, https://doi.org/10.1039/c7ra12310h.
[262] H. Sepehrian, M. Samadfam, Z. Asadi, Studies on the recovery of uranium from nuclear industrial effluent using nanoporous silica adsorbent, Int. J. Environ. Sci. Technol. 9 (2012) 629–636, https://doi.org/10.1007/s13762-012-0065-3.
[263] K. Guo, F. Han, Z. Arslan, J. McComb, X. Mao, R. Zhang, S. Sudarson, H. Yu, Adsorption of Cs from water on surface-modified MCM-41 mesosilicate, water, Air. Soil Pollut. 226 (2015), https://doi.org/10.1007/s11270-015-2565-5.
[264] A. Benhamou, M. Baudu, Z. Derriche, J.P. Basly, Aqueous heavy metals removal on amine-functionalized Si-MCM-41 and Si-MCM-48, J. Hazard Mater. 171 (2009) 1001–1008, https://doi.org/10.1007/s10750-011-0851-9.
[265] G. Bayramoglu, M.Y. Arica, MCM-41 silica particles grafted with polyacrylonitrile: modification in to amidoxime and carboxyl groups for enhanced uranium removal from aqueous medium, Microporous Mesoporous Mater. 226 (2016) 117–124, https://doi.org/10.1016/j.micromeso.2015.12.040.
[266] M. Ghorbani, S.M. Nowee, Kinetic study of Pb(II) and Ni(II) adsorption onto MCM-41 amine- functionalized nano particle, Adv. Environ. Technol. 2 (2016) 101–104.
[267] H. Faghihian, M. Naghavi, Synthesis of amine-functionalized MCM-41 and MCM-48 for removal of heavy metal ions from aqueous solutions, Separ. Sci. Technol. 49 (2014) 214–220, https://doi.org/10.1080/01496395.2013.819516.
[268] H. Ebrahimzadeh, N. Tavassoli, O. Sadeghi, M.M. Amini, S. Vahidi, S.M. Aghigh, E. Moazzen, Extraction of nickel from soil, water, fish, and plants on novel pyridine-functionalized MCM-41 and MCM-48 nanoporous silicas and its subsequent determination by FAAS, Food Anal. Methods. 5 (2012) 1070–1078, https://doi.org/10.1007/s12161-011-9344-8.
[269] K. Parida, K.G. Mishra, S.K. Dash, Adsorption of toxic metal ion Cr(VI) from aqueous state by TiO2-MCM-41: equilibrium and kinetic studies, J. Hazard Mater. 241–242 (2012) 395–403, https://doi.org/10.1016/j.jhazmat.2012.09.052.
[270] X. Chen, K.F. Lam, K.L. Yeung, Selective removal of chromium from different aqueous systems using magnetic MCM-41 nanosorbents, Chem. Eng. J. 172 (2011) 728–734, https://doi.org/10.1016/j.cej.2011.06.042.
[271] X. Li, C. Han, W. Zhu, W. Ma, Y. Luo, Y. Zhou, J. Yu, K. Wei, Cr(VI) removal from aqueous by adsorption on amine-functionalized mesoporous silica prepared from silica fume, J. Chem. 2014 (2014), https://doi.org/10.1155/2014/765856.
[272] W. Kaewprachum, S. Wongsakulphasatch, W. Kiatkittipong, A. Striolo, C.K. Cheng, S. Assabumrungrat, SDS modified mesoporous silica MCM-41 for the adsorption of Cu2+, Cd2+, Zn2+ from aqueous systems, J. Environ. Chem. Eng. (2019) 102920.
[273] M. Puanngam, F. Unob, Preparation and use of chemically modified MCM-41 and silica gel as selective adsorbents for Hg(II) ions, J. Hazard Mater. 154 (2008) 578–587, https://doi.org/10.1016/j.jhazmat.2007.10.090.
[274] D. Pérez-Quintanilla, A. Sánchez, I. del Hierro, M. Fajardo, I. Sierra, Preparation, characterization, and Zn2+adsorption behavior of chemically modified MCM-41 with 5-mercapto-1-methyltetrazole, J. Colloid Interface Sci. 313 (2007) 551–562, https://doi.org/10.1016/j.jcis.2007.04.063.
[275] D. Pérez-Quintanilla, I. Del Hierro, M. Fajardo, I. Sierra, Preparation of 2-mercaptobenzothiazole-derivatized mesoporous silica and removal of Hg(II) from aqueous solution, J. Environ. Monit. 8 (2006) 214–222, https://doi.org/10.1039/b507983g.
[276] A. Mehdinia, M. Akbari, T. Baradaran Kayyal, M. Azad, High-efficient mercury removal from environmental water samples using di-thio grafted on magnetic mesoporous silica nanoparticles, Environ. Sci. Pollut. Res. 22 (2015) 2155–2165, https://doi.org/10.1007/s11356-014-3430-6.
[277] G. Mohammadnezhad, S. Abad, R. Soltani, M. Dinari, Study on thermal, mechanical and adsorption properties of amine-functionalized MCM-41/PMMA and MCM-41/PS nanocomposites prepared by ultrasonic irradiation, Ultrason.

Sonochem. 39 (2017) 765–773, https://doi.org/10.1016/j.ultsonch.2017.06.001.
[278] A.K. Thakur, G.M. Nisola, L.A. Limjuco, K.J. Parohinog, R. Eliseo, C. Torrejos, V.K. Shahi, W. Chung, Polyethylenimine-modi fi ed mesoporous silica adsorbent for simultaneous removal of Cd(II) and Ni (II) from aqueous solution, J. Ind. Eng. Chem. 49 (2017) 133–144.
[279] W. Zhu, J. Wang, D. Wu, X. Li, Y. Luo, C. Han, W. Ma, S. He, Investigating the heavy metal adsorption of mesoporous silica materials prepared by microwave synthesis, Nanoscale Res. Lett. 12 (2017), https://doi.org/10.1186/s11671-017-2070-4.
[280] P.P. Martin, M.F. Agosto, J.F. Bengoa, N.A. Fellenz, Zinc and Chromium elimination from complex aqueous matrices using a unique aminopropyl-modi fi ed MCM-41 sorbent : temperature , kinetics and selectivity studies, Biochem. Pharmacol. 5 (2017) 1210–1218, https://doi.org/10.1016/j.jece.2017.02.003.
[281] Y. Wu, S. Yang, M. Zhang, A. Aierken, Y. Wu, Abatement of Cr(VI) and As(III) by MnO2 loaded MCM-41 in wastewater treatment, Korean J. Chem. Eng. 32 (2015) 1667–1677, https://doi.org/10.1007/s11814-014-0352-4.
[282] Y. Wu, Y. Jin, J. Cao, P. Yilihan, Y. Wen, J. Zhou, Optimizing adsorption of arsenic (III) by NH2-MCM-41 using response surface methodology, J. Ind. Eng. Chem. 20 (2014) 2792–2800, https://doi.org/10.1016/j.jiec.2013.11.009.
[283] M. Vasudevan, P.L. Sakaria, A.S. Bhatt, H.M. Mody, H.C. Bajaj, Effect of concentration of aminopropyl groups on the surface of MCM-41 on adsorption of Cu2+, Ind. Eng. Chem. Res. 50 (2011) 11432–11439, https://doi.org/10.1021/ie201448q.
[284] T. Areerob, S. Chiarakorn, N. Grisdanurak, Enhancement of gaseous BTEX adsorption on RH-MCM-41 by chlorosilanes, Sains Malays. 44 (2015) 429–439, https://doi.org/10.17576/jsm-2015-4403-15.
[285] N. Hazrati, M. Abdouss, A. Vahid, A.A. Miran Beigi, A. Mohammadalizadeh, Removal of H2S from crude oil via stripping followed by adsorption using ZnO/MCM-41 and optimization of parameters, Int. J. Environ. Sci. Technol. 11 (2014) 997–1006, https://doi.org/10.1007/s13762-013-0465-z.
[286] Z. Li, Y. Liu, X. Yang, Y. Xing, Q. Yang, R.T. Yang, Adsorption thermodynamics and desorption properties of gaseous polycyclic aromatic hydrocarbons on mesoporous adsorbents, Adsorption 23 (2017) 361–371, https://doi.org/10.1007/s10450-017-9863-8.
[287] J. Zhou, H. Zhao, J. Li, Y. Zhu, J. Hu, H. Liu, Y. Hu, CO2 capture on micro/mesoporous composites of (zeolite A)/(MCM-41) with Ca2+ located: computer simulation and experimental studies, Solid State Sci. 24 (2013) 107–114, https://doi.org/10.1016/j.solidstatesciences.2013.07.008.
[288] X. Wang, L. Chen, Q. Guo, Development of hybrid amine-functionalized MCM-41 sorbents for CO2 capture, Chem. Eng. J. 260 (2015) 573–581, https://doi.org/10.1016/j.cej.2014.08.107.
[289] N.E. Tari, A. Tadjarodi, J. Tamnanloo, S. Fatemi, Synthesis and property modification of MCM-41 composited with Cu(BDC) MOF for improvement of CO2 adsorption Selectivity, J. CO2 Util. 14 (2016) 126–134, https://doi.org/10.1016/j.jcou.2016.04.008.
[290] L.S. de Carvalho, E. Silva, J.C. Andrade, J.A. Silva, M. Urbina, P.F. Nascimento, F. Carvalho, J.A. Ruiz, Low-cost mesoporous adsorbents amines-impregnated for CO2 capture, Adsorption 21 (2015) 597–609, https://doi.org/10.1007/s10450-015-9710-8.
[291] J. Zhang, H. Song, Y. Chen, T. Hao, F. Li, D. Yuan, X. Wang, L. Zhao, J. Gao, Amino-modified molecular sieves for adsorptive removal of H2S from natural gas, RSC Adv. 8 (2018) 38124–38130, https://doi.org/10.1039/C8RA06859C.
[292] Z. Li, Y. Liu, X. Yang, Y. Xing, C.J. Tsai, M. Meng, R.T. Yang, Performance of mesoporous silicas and carbon in adsorptive removal of phenanthrene as a typical gaseous polycyclic aromatic hydrocarbon, Microporous Mesoporous Mater. 239 (2017) 9–18, https://doi.org/10.1016/j.micromeso.2016.09.027.
[293] P.J. Branton, P.G. Hall, M. Treguer, K.S.W. Sing, Adsorption of carbon dioxide, sulfur dioxide and water vapour by MCM-41, a model mesoporous adsorbent, J. Chem. Soc. Faraday. Trans. 91 (1995) 2041–2043, https://doi.org/10.1039/FT9959102041.
[294] N. Pal, T. Kim, J. Park, E. Cho, Synthesis of ordered Ca- and Li-doped mesoporous silicas for H2 and CO2 adsorption at ambient temperature and pressure, RSC Adv. (2018) 35294–35305 doi:2018/RA/C8RA05772A.
[295] Y. Belmabkhout, A. Sayari, Adsorption of CO2from dry gases on MCM-41 silica at ambient temperature and high pressure. 2: adsorption of CO2/N2, CO2/CH4and CO2/H2binary mixtures, Chem. Eng. Sci. 64 (2009) 3729–3735, https://doi.org/10.1016/j.ces.2009.05.039.
[296] K.J. Edler, P.A. Reynolds, P.J. Branton, F.R. Trouw, J.W. White, Structure and dynamics of hydrogen sorption in mesoporous MCM-41, Faraday Trans. 93 (1997) 1667–1674, https://doi.org/10.1039/a607878h.
[297] P. Carraro, V. Elías, A.A.G. Blanco, K. Sapag, G. Eimer, M. Oliva, Study of hydrogen adsorption properties on MCM- 41 mesoporous materials modified with nickel, Int. J. Hydrogen Energy 39 (2014) 8749–8753.
[298] Y. Belmabkhout, R. Serna-Guerrero, A. Sayari, Adsorption of CO2-containing gas mixtures over amine-bearing pore-expanded MCM-41 silica: application for gas purificatio, Ind. Eng. Chem. Res. 49 (2010) 359–365, https://doi.org/10.1021/ie900837t.
[299] M.N. Barbosa, A.S. Araujo, L.P.F.C. Galvão, E.F.B. Silva, A.G.D. Santos, G.E. Luz, V.J. Fernandes, Carbon dioxide adsorption over DIPA functionalized MCM-41 and SBA-15 molecular sieves, J. Therm. Anal. Calorim. 106 (2011) 779–782, https://doi.org/10.1007/s10973-011-1398-8.
[300] P.J. Carrott, a. Neimark, M.M. Ribeiro Carrott, a.J. Candeias, P. Ravikovitch, a. Sequeira, Adsorption of nitrogen, neopentane, n-hexane, benzene and methanol for the evaluation of pore sizes in silica grades of MCM-41, Microporous Mesoporous Mater. 47 (2001) 323–337, https://doi.org/10.1177/0886260513487988.
[301] K. Machowski, P. Kuśtrowski, B. Dudek, M. Michalik, Elimination of ketone vapors by adsorption on spherical MCM-41 and MCM-48 silicas decorated with thermally activated poly(furfuryl alcohol), Mater. Chem. Phys. 165 (2015) 253–260, https://doi.org/10.1016/j.matchemphys.2015.09.026.
[302] Y. Liu, Z. Li, X. Yang, Y. Xing, C. Tsai, Q. Yang, Z. Wang, R.T. Yang, Performance of mesoporous silicas (MCM-41 and SBA-15) and carbon (CMK-3) in the removal of gas-phase naphthalene: adsorption capacity, rate and regenerability, RSC Adv. 6 (2016) 21193–21203, https://doi.org/10.1039/c5ra27289k.